DEPARTMENT OF COMMERCE
FREDERICK H. MUELLER, Secretary

WEATHER BUREAU
F. W. REICHELDERFER, Chief

MONTHLY WEATHER REVIEW

JAMES E. CASKEY, JR., Editor

Volume 88
Number 2

FEBRUARY 1960

Closed April 15, 1960
Issued May 15, 1960

A PRELIMINARY REPORT ON OZONE OBSERVATIONS AT LITTLE AMERICA, ANTARCTICA[1]

H. WEXLER, W. B. MORELAND, AND W. S. WEYANT

U. S. Weather Bureau, Washington, D. C.

[Manuscript received December 11, 1959; revised January 28, 1960]

ABSTRACT

Summaries of ozone measurements made at Little America, Antarctica during 1957 and 1958 are presented. Data include both total ozone observations made with a Dobson Ozone Spectrophotometer and surface ozone concentrations measured with the automatic ozone recorder developed by Regener. Wind and ozone roses were constructed to examine the variation of surface ozone with wind direction, and in addition the net meridional transport of surface ozone was computed for each month for a year.

The computed northward transport of surface ozone during the winter months of June through September suggests a model for atmospheric circulation in the Antarctic. Assuming no ozone is created or destroyed by photochemical or other means during this dark period and that Little America is representative of its latitude, steady-state conditions require that the low-level outflow of ozone be compensated by inflow at other levels. Both the lower stratospheric circumpolar jet inhibiting meridional transport and the stability of the Antarctic stratosphere inhibiting downward vertical transport lead us to ascribe the principal ozone influx to the troposphere above the surface layer. Computations of the tropospheric ozone concentrations required to replace the low-level loss of ozone, using Rubin's values for the vertical distribution of the tropospheric mass transports, are in good agreement with the observations made by ozonesonde at Halley Bay.

It thus appears that some of the ozone manufactured in the sunlit stratosphere of lower latitudes which enters the troposphere through the tropopause gap associated with the mid-latitude jet stream is transported into the Antarctic by winds of the vigorous winter storms which move around and into the continent, and finally sinks and then flows northward again as part of the 2- to 3-km. thick surface layer.

1. INTRODUCTION

Beginning in early 1957 measurements of surface ozone concentration and total ozone were carried out at the US-IGY Little America Station, located on the shelf ice 2½ miles south of the Ross Sea, Antarctica (78°11′S., 162°10′W., 44 meters m.s.l.). See figure 1. Air which reaches the Little America Station from east through south to west has traveled for thousands of miles over a snow field, lying on ice hundreds of feet thick. Winds from west-northwest clockwise to east-northeast have moved over predominantly sea-ice, generally not more than 10 feet thick, except during January to April when mostly open ocean or very thin ice is found. In September-October the sea-ice has its greatest extension, reaching about 1,000 miles northward. The only plant life, lichens, is found on the nearest exposed rock of the Rockefeller Mountains, 70 miles east of Little America.

To take advantage of this unique high-latitude site, a program of measurement of total ozone content in the vertical column by means of the Dobson Ozone Spectrophotometer was begun in February 1957 by W. B. Moreland and continued in 1958 by W. S. Weyant. The surface ozone program was started in late March 1957 by B. W. Harlin, also of the U.S. Weather Bureau, who installed the automatic ozone recorder developed by

[1] Presented in condensed form at the International Conference on Atmospheric Ozone—Oxford Symposium, July 1959 and at the Antarctic Symposium of Buenos Aires, November 1959.

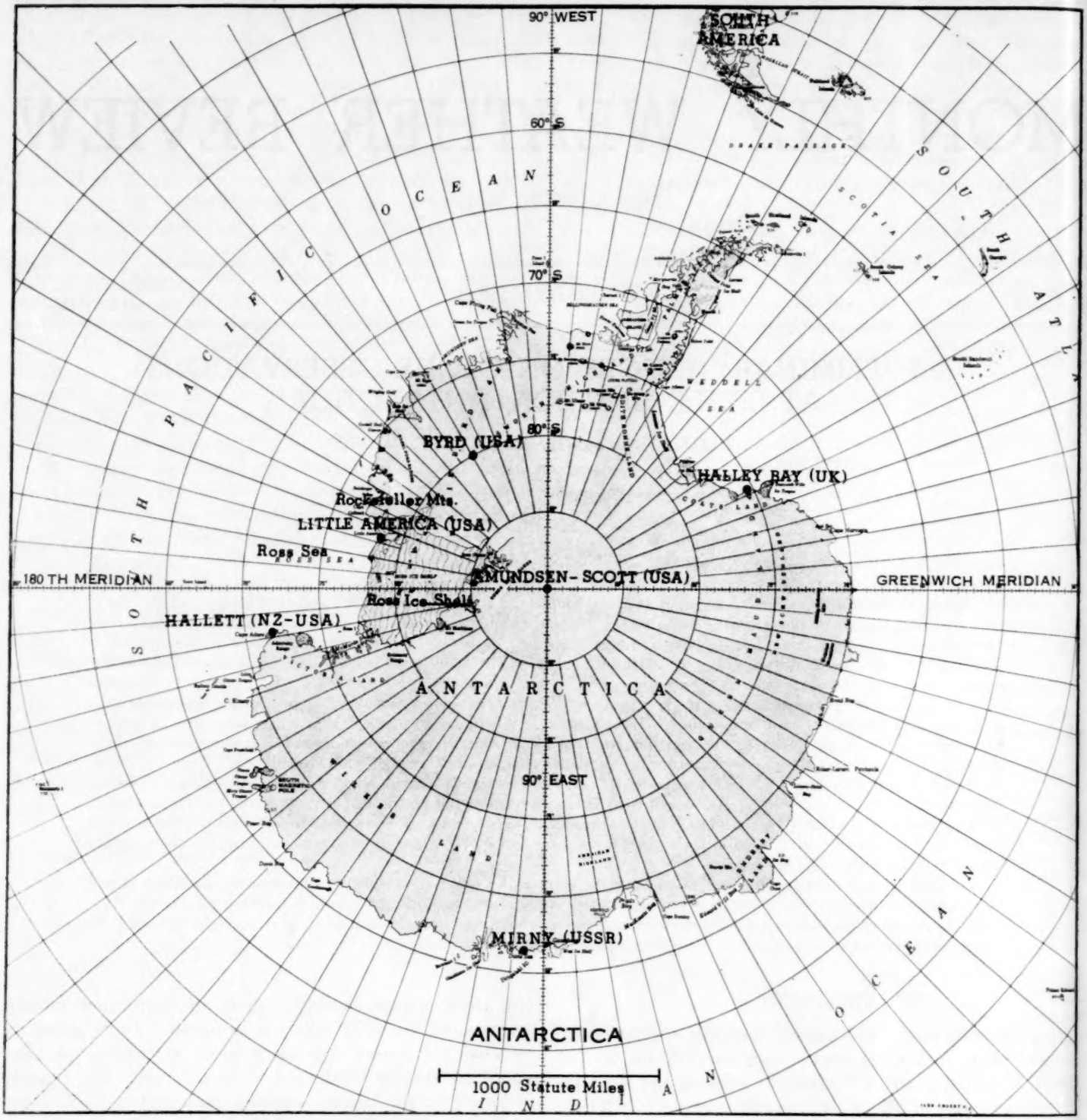

FIGURE 1.—Map of Antarctica showing sites mentioned in text.

Regener [9]; measurements were made from December 1957 through October 1958 by W. S. Weyant.

2. EXPOSURE OF INSTRUMENTS AND METHODS OF OBSERVATION

Total ozone—Measurements of total ozone were made with Dobson Ozone Spectrophotometer Number 37 located in the "Aurora Tower" (fig. 2). The instrument was so mounted that the sun-director was located under a dome which could be rotated 360 degrees. A section of the dome could be opened to permit either direct sun or zenith sky observations.

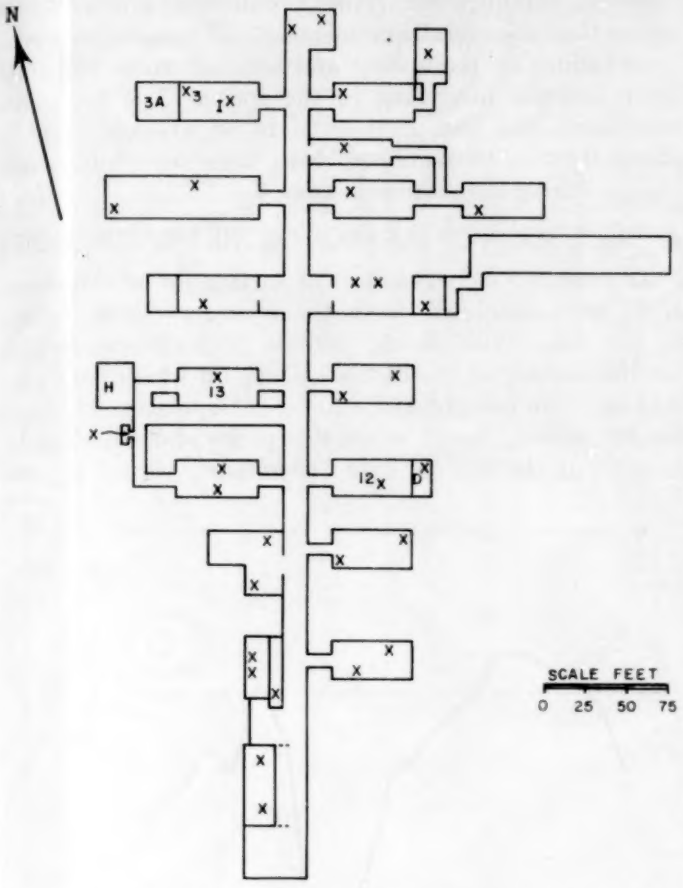

FIGURE 2.—Plan of buildings at Little America V, Antarctica. No. 3 is meteorology building. Intake for air for surface ozone analyzer, indicated by "I", is located about 4½ ft. above building roof. No. 12 is aurora-air glow building. Dobson ozone spectrophotometer, indicated by "D", is on aurora tower at rear of building 12. The roof of the tower is about 25 ft. above the general roof level of the other buildings. Building marked "H" behind No. 13 is the hydrogen shelter where rawinsonde balloons are inflated and released. Smoke sources are indicated by the letter "X".

A detailed description of the instrument and observational procedures has been given by Dobson [3]. At Little America the wavelength pairs designated "A", "B", "C", and "D" [3] were employed whenever feasible. These wavelengths are:

Wavelength pair:	A	B	C	D
Short (Å.)	3055	3088	3114.5	3176
Long (Å.)	3254	3291	3324	3398

During the spring and autumn months the "A" and "B" wavelengths frequently could not be used due to the weak light intensity caused by the low elevation of the sun. During the polar night measurements were made using the moon as a light source; because of the low sensitivity of the instrument only "D" wavelengths could be employed then.

Ozone values were based upon the standard "AD" reduction when the "A" wavelengths were obtainable; otherwise, the values were obtained from "CD" measurements. Zenith cloud values were not utilized in obtaining averaged monthly ozone amounts since a comparison of zenith cloud and direct sun values showed that they were not compatible. All the ozone values must be considered provisional until the instrument is recalibrated upon its return to the United States.

Surface ozone—Figure 2 also shows the physical location of the air intake for the surface ozone analyzer, and nearby sources of atmospheric pollution in the camp.

The air intake was located about 4½ feet above the roof of the Meteorology Office, and at a lesser but variable distance above the snow which covered the roof except for the brief summer season. Each of the permanent buildings contains two diesel oil heaters, with stovepipes discharging the combustion by-products at about 6 feet above the building roofs. As can be seen from the diagram the main part of the camp, and hence the maximum amount of air pollution from this source, is located in the quadrant between east-southeast and south-southwest relative to the air intake.

The glass tube of the intake itself curves around at the top to end in an inverted glass beaker about 3 inches in diameter, which is packed with glass wool to prevent entrance of particulate matter into the ozone measuring device. It was noted that only a few hours' exposure of fresh glass wool in the beaker was sufficient to collect enough soot to be visible, and after about one day the intake surface of the glass wool became completely blackened. The glass wool was changed only when the air flow through the measuring device dropped, not more often than once a month at best. Since replacing the soot-encrusted wool with clean wool did not result in any noticeable change in the instrument readings, it does not appear likely that there was a significant local effect on surface ozone concentration.

3. DISCUSSION OF TOTAL OZONE OBSERVATIONS

As direct sun observations using the "A" and "D" pairs of wavelengths give the most reliable values of total ozone, these values were used on days when such observations were possible. On other days when sun observations using the "CD" pairs of wavelengths were obtained, these ozone values were used, after applying a correction to make them more nearly compatible with the "AD" observations (see next paragraph). Finally, with only the full moon or with very low sun, when neither of the above types of observations was possible, the focused image values on the "D" wavelengths only were used. In all of the computed values, the ozone absorption coefficients as determined by Vigroux [12] and listed by Dobson [3] were the ones applied.

There were several occasions when readings on both the "AD" and "CD" pairs of wavelengths were obtained at nearly the same time, so that a comparison of the two types of readings was possible. Fifty-four such occasions were analyzed, and it was found that on the average the "CD" readings gave 0.055 cm. lower values of ozone than the "AD"

TABLE 1.—*Mean total ozone observations at Little America V, Antarctica, in cm. of pure ozone, reduced to standard temperature and pressure. Number of days' observations in parentheses.*

Month	1957	1958	Combined	Remarks
January	none	0.314 (13)	0.314 (13)	Direct sun AD
February	0.299 (2)	.314 (5)	.310 (7)	Direct sun AD
March	.333 (15)	.335 (1)	.334 (16)	Mostly FIS CD or D
April	.266 (4)	none	.266 (4)	FI moon on D
May	.395 (2)	.349 (1)	.380 (3)	FI moon on D
June	.480 (2)	none	.480 (2)	FI moon on D
July	.346 (3)	.433 (1)	.368 (4)	FI moon on D
August	.536 (2)	none	.536 (2)	FI moon on D
September	.334 (17)	none	.334 (17)	Mostly FIS CD or D
October	.384 (15)	.353 (8)	.373 (23)	Mostly direct sun AD or CD
November	.421 (21)	.399 (1)	.420 (22)	Direct sun AD
December	.316 (3)	none	.316 (3)	Direct sun AD
Mean for all observations 0.360 (116)				

FIS=focused image observation on the sun.
FI moon=focused image observation on the moon.

readings, with a standard deviation in the differences of 0.009 cm. A graph of the 54 differences plotted against air mass and against the "AD" values showed no apparent relationship of the differences to either parameter. All of the "CD" values used in this report were corrected by adding 0.055 to the computed ozone value. (Qualitatively the values from the "D" wavelengths alone also seem lower than the "AD" values for the same time, but in view of the much greater variability of the differences no correction factor was applied to these readings.)

Table 1 shows the mean ozone values obtained by the above methods of observation for each month for 1957 and 1958 and the combined data. Figures in parentheses following each mean value give the number of days' observations on which the mean was based. Figure 3 is a graph of the combined values, with the number of days entered in the plotted circle.

The dark-season observations are too few in number and too variable in value to permit any firm conclusions as to winter atmospheric ozone content over Little America, although their mean indicates winter values higher than the overall annual mean. The more numerous observations in the spring and summer show the total ozone content increasing in the spring to a November maximum, and then decreasing to an average value of about 0.32 in the summer, with little month-to-month change during the summer season.

4. DISCUSSION OF SURFACE OZONE MEASUREMENTS

The mean hourly readings of surface ozone concentrations were extracted from the recorder charts. Gaps in the data exist during periods of malfunctioning or nonfunctioning of the device. Days on which data were missing were completed by linear interpolation of values for the missing hours, when this period did not exceed 6 hours and the change over the missing period was not

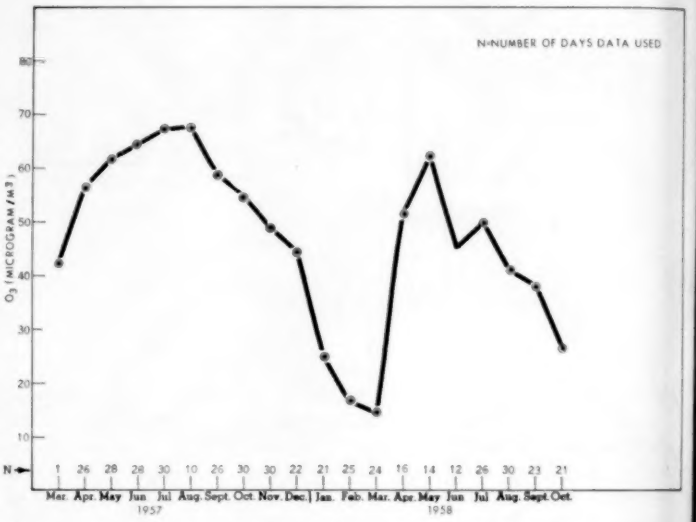

FIGURE 4.—Little America Station monthly average surface ozone concentrations, March 1957 through October 1958.

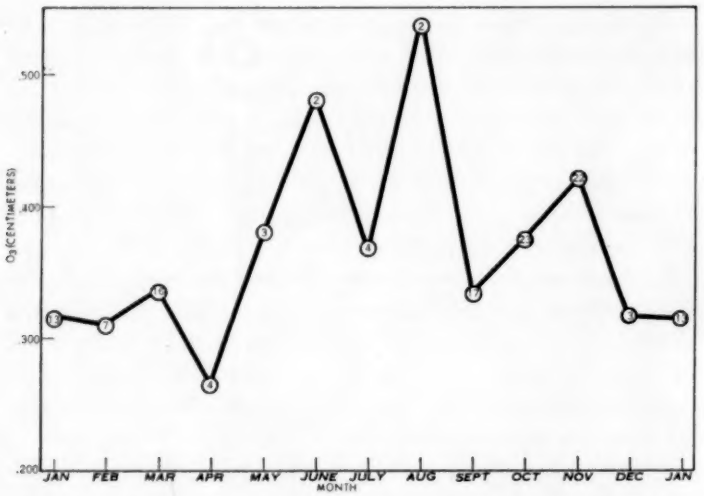

FIGURE 3.—Little America Station total ozone, average of 1957 and 1958. Within circle is number of days' observations.

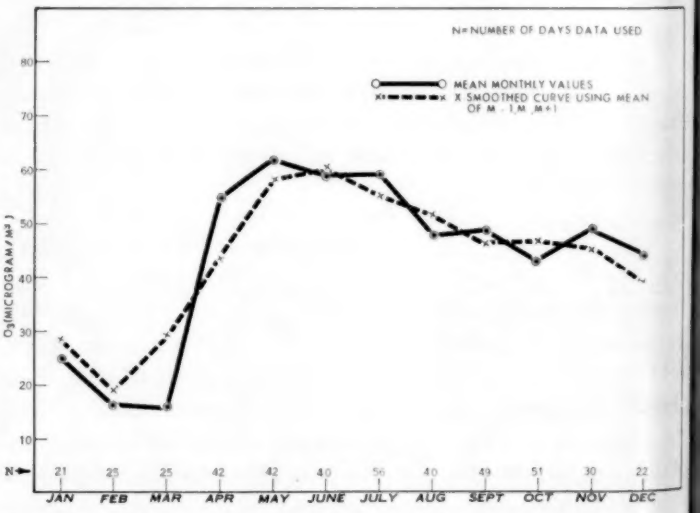

FIGURE 5.—Little America Station monthly average surface ozone concentrations—combined 1957–58 data.

TABLE 2.—*Daily values of surface ozone concentration at Little America V, Antarctica in micrograms m.$^{-3}$ Interpolated values are enclosed in parentheses. Means are of observed values only.*

Day (GMT)	1957 Mar.	Apr.	May	June	July	Aug.	Sept.	Oct.	Nov.	Dec.	1958 Jan.	Feb.	Mar.	Apr.	May	June	July	Aug.	Sept.	Oct.
1	.....	52.0	61.9	66.2	65.8	65.5	(65.6)	(45.6)	52.7	40.7	21.5	16.5	21.1	(44.7)	(75.0)	(38.5)	(50.6)	49.3	(50.6)	29.9
2	.....	(51.0)	59.3	63.3	66.9	69.8	(65.3)	48.8	52.7	41.4	22.1	12.0	21.9	(46.3)	81.1	35.1	(58.1)	40.6	53.1	30.4
3	.....	(50.1)	57.3	68.5	62.2	72.2	(64.9)	45.3	51.9	39.1	27.8	13.8	17.6	(47.8)	(77.8)	(36.7)	65.7	26.5	(49.5)	(30.4)
4	.....	49.1	66.1	71.1	64.7	66.3	(64.5)	42.3	53.5	42.0	29.3	20.9	23.0	(49.4)	(74.5)	(38.3)	50.4	36.1	45.8	30.4
5	.....	52.1	65.1	67.8	61.9	53.6	64.2	51.7	52.1	41.6	24.4	16.2	21.0	(51.0)	(71.3)	(39.9)	53.0	39.4	42.1	23.9
6	.....	53.5	60.2	(70.6)	75.9	(58.2)	63.7	61.8	57.5	41.9	19.2	18.5	17.5	(52.5)	(68.1)	(41.6)	(49.3)	33.8	37.5	(25.6)
7	.....	53.5	60.0	73.5	71.8	62.8	64.1	62.0	57.8	35.3	14.1	22.7	12.0	(54.1)	(64.8)	(43.2)	45.7	41.9	38.0	(27.3)
8	.....	53.6	62.8	74.4	69.5	66.9	64.2	59.1	60.3	(37.5)	19.1	21.9	8.3	(55.7)	(61.5)	(44.8)	41.7	44.1	36.3	29.0
9	.....	56.1	52.4	72.4	68.7	69.4	66.9	61.6	53.7	(39.8)	(17.8)	16.8	9.4	(57.3)	(58.3)	(46.5)	41.0	47.3	(36.5)	23.0
10	.....	52.1	61.4	72.3	68.2	72.9	66.4	59.0	53.0	42.0	16.4	19.2	4.8	58.9	(55.0)	(48.1)	50.6	42.4	(36.8)	(22.5)
11	.....	60.1	55.4	72.5	69.9	73.2	69.6	57.0	49.7	46.3	26.2	13.3	7.9	65.2	51.7	(49.7)	57.1	33.8	37.0	(22.1)
12	.....	58.3	62.3	64.9	68.2	(72.8)	73.6	65.3	49.2	47.8	31.2	14.4	7.6	68.3	53.0	51.3	58.0	32.9	(39.0)	(21.6)
13	.....	59.7	59.0	56.6	70.0	(72.5)	66.0	58.3	49.5	49.6	(31.4)	18.2	4.3	65.1	(57.5)	40.5	49.0	41.0	40.9	(21.2)
14	.....	62.0	57.8	61.4	(67.6)	(72.1)	58.8	60.9	52.0	48.2	(31.7)	20.8	6.7	60.0	58.0	43.9	44.5	41.7	(44.8)	(20.7)
15	.....	61.9	55.5	57.1	65.3	(71.7)	56.2	56.7	53.0	37.4	(31.9)	15.7	2.8	57.7	59.6	(53.4)	53.0	44.1	(48.8)	20.2
16	.....	56.4	58.1	59.2	65.6	(71.4)	58.8	53.3	55.8	37.8	(32.1)	12.0	(3.6)	51.7	61.4	62.9	59.2	43.7	52.7	24.2
17	.....	56.6	57.2	56.7	68.1	(71.0)	50.4	44.7	55.2	(39.3)	(32.4)	8.3	(4.4)	46.2	58.9	37.0	54.3	42.0	44.2	22.8
18	.....	(55.7)	61.6	54.9	64.4	(70.7)	64.4	59.9	46.2	40.7	(32.6)	9.5	(5.3)	40.9	65.4	30.6	51.3	43.4	46.5	22.5
19	.....	(54.7)	58.9	51.2	70.6	(70.3)	62.1	53.8	46.6	36.0	(32.9)	9.7	(6.1)	43.0	67.4	43.1	53.8	43.1	37.7	24.8
20	.....	53.8	61.2	44.5	69.9	(69.9)	65.8	57.9	42.0	42.0	33.1	10.3	6.9	49.2	60.2	(49.5)	47.5	42.9	42.6	22.1
21	.....	51.2	66.5	(57.8)	64.0	(69.6)	59.6	61.4	45.9	40.1	30.9	15.5	10.9	51.9	60.4	55.8	48.6	(40.1)	41.2	28.3
22	.....	52.6	65.3	71.0	60.2	(69.2)	51.1	57.7	37.0	51.8	37.4	17.9	7.5	47.9	63.4	59.5	51.0	37.4	22.3	31.7
23	.....	57.8	66.9	67.6	65.8	(68.9)	43.1	49.7	41.8	(54.5)	29.2	21.3	5.9	38.2	64.3	45.0	42.9	39.8	33.8	37.3
24	.....	58.0	65.7	67.5	63.9	(68.5)	48.0	45.8	43.4	(57.2)	31.2	(20.5)	8.5	41.2	66.5	(43.4)	39.5	34.3	31.7	28.8
25	.....	59.9	64.8	63.3	67.7	(68.1)	45.8	48.4	45.4	59.9	21.1	(19.8)	9.2	38.6	(63.0)	(41.8)	40.7	39.1	31.5	(27.2)
26	.....	60.7	61.6	58.9	62.8	(67.8)	48.5	53.6	40.9	53.3	21.0	(19.0)	(22.5)	(44.7)	(59.5)	(40.3)	45.3	46.8	29.4	(25.5)
27	42.1	55.1	69.9	67.7	66.4	(67.4)	52.9	47.8	41.8	55.6	19.8	18.3	35.7	(50.8)	(56.0)	(38.7)	41.4	38.9	32.9	23.9
28	(44.1)	60.8	68.4	67.4	68.4	(67.1)	58.1	51.3	41.3	(48.8)	22.6	21.8	39.8	(56.8)	(52.5)	(37.1)	48.0	47.4	28.1	24.8
29	(46.1)	59.1	(67.8)	64.7	66.9	(66.7)	50.6	51.4	33.9	(42.0)	(21.5)		40.0	(62.9)	(49.0)	35.5	(52.5)	43.8	33.1	28.8
30	(48.0)	63.9	(67.3)	66.4	68.1	(66.3)	42.3	54.6	40.4	(35.2)	(20.4)		(41.6)	(69.0)	(45.5)	(43.0)	(56.9)	44.1	32.9	26.2
31	(50.0)		(66.7)		67.8	(66.0)		58.7		(28.4)	19.3		(43.1)		(42.0)		61.4	48.1		24.2
Mean	42.1	56.5	61.6	64.4	67.0	67.3	58.3	54.7	48.6	44.1	24.6	16.2	14.6	51.5	62.1	45.0	49.8	41.0	37.9	26.5

TABLE 3.—*Hourly mean values of surface ozone at Little America V, Antarctica, in micrograms m.$^{-3}$ N is the number of complete days' data for each month.*

Hour ending (GMT)	1957 Mar.	Apr.	May	June	July	Aug.	Sept.	Oct.	Nov.	Dec.	1958 Jan.	Feb.	Mar.	Apr.	May	June	July	Aug.	Sept.	Oct.	443-day mean
01	42.6	54.6	61.1	62.9	65.0	66.3	51.3	53.2	48.0	42.9	24.5	15.7	15.1	52.6	62.1	45.9	49.9	41.1	37.4	25.4	45.9
02	40.5	54.4	61.1	62.2	64.6	65.9	51.4	52.8	47.4	43.1	24.6	15.7	15.1	52.3	62.1	46.3	50.0	40.8	37.4	25.8	45.7
03	38.4	54.6	60.9	61.9	64.2	65.0	52.0	52.8	47.4	42.8	24.5	15.2	14.4	51.6	61.5	47.1	50.3	41.2	37.0	26.5	45.6
04	38.4	55.4	62.1	63.0	64.5	64.6	53.5	53.5	47.3	41.9	24.8	15.2	13.6	51.2	61.0	47.1	50.1	40.9	36.3	26.2	45.8
05	40.5	56.0	61.8	64.1	66.1	66.2	55.0	53.8	47.7	41.7	25.5	15.1	13.7	51.0	60.5	47.5	50.2	41.2	36.7	27.0	46.2
06	40.5	56.7	61.6	64.4	66.5	66.5	56.4	54.3	47.6	42.0	24.9	15.1	13.8	50.8	59.9	46.0	50.2	41.5	37.0	27.6	46.4
07	40.5	57.1	61.6	65.3	66.9	66.7	58.3	53.9	47.8	42.7	25.0	14.9	14.5	50.7	60.5	46.0	50.4	41.0	37.4	27.9	46.7
08	40.5	57.9	60.9	65.1	67.6	66.7	59.9	54.8	47.8	43.1	24.3	15.1	14.0	51.0	60.2	46.2	50.7	40.8	37.4	27.2	46.9
09	42.6	57.4	61.2	65.2	67.4	66.4	60.8	54.5	48.0	42.6	24.6	15.2	14.0	50.6	59.8	45.0	50.3	40.2	38.1	26.1	46.8
10	42.6	57.7	60.6	64.6	67.6	67.6	61.1	54.5	48.3	42.9	24.2	15.4	14.2	51.3	59.6	44.3	50.0	40.5	38.7	26.3	46.8
11	42.6	57.8	61.6	65.5	68.3	68.3	61.5	54.8	48.6	44.1	24.6	15.4	14.5	51.6	60.5	43.7	50.0	40.1	38.3	26.2	47.2
12	42.6	57.9	62.6	66.6	68.7	68.5	62.1	54.9	48.9	45.5	24.8	15.2	14.6	51.3	61.2	44.8	50.4	40.4	39.0	27.1	47.6
13	42.6	57.8	62.2	67.2	68.9	67.8	62.7	56.5	49.1	46.1	24.8	16.2	14.6	51.6	62.3	44.8	50.2	40.9	39.2	26.6	47.9
14	42.6	58.0	62.7	66.6	68.8	69.9	63.7	56.5	49.3	45.6	24.4	17.1	14.6	51.2	63.0	45.8	49.9	41.0	39.7	27.3	48.1
15	44.6	58.1	63.1	66.2	68.8	69.9	63.3	56.6	49.7	45.7	24.6	17.8	15.2	51.4	64.1	46.7	49.6	41.1	39.4	27.5	48.3
16	44.6	58.2	63.3	65.0	68.6	69.9	63.8	56.9	50.0	45.6	24.2	17.8	14.5	51.6	64.8	45.6	49.7	40.9	38.9	27.4	44.2
17	46.9	57.6	61.9	65.1	67.9	68.8	63.2	56.4	50.1	45.4	23.7	18.3	15.0	52.0	64.8	45.6	49.3	41.0	39.1	27.0	48.0
18	46.9	56.9	62.5	65.4	68.2	68.3	62.1	56.1	49.9	44.9	24.1	18.1	15.1	52.4	63.6	44.4	49.6	41.2	39.2	26.8	47.8
19	46.9	55.3	62.1	65.3	68.1	67.9	61.5	55.8	49.6	44.9	24.1	17.5	15.4	52.3	63.8	43.1	49.7	41.5	38.8	27.0	47.6
20	42.6	55.0	61.3	64.0	67.6	66.9	59.9	55.5	49.0	45.1	24.8	16.9	14.7	52.2	63.7	42.9	49.4	41.6	37.9	26.3	47.1
21	40.5	55.6	60.5	62.8	66.2	66.4	57.0	54.2	48.8	44.6	24.6	16.9	14.9	52.0	62.7	41.9	49.2	42.1	37.0	26.0	46.5
22	40.5	55.8	59.7	62.4	65.8	66.9	54.7	53.0	48.6	44.5	24.9	16.9	15.2	51.0	63.2	42.9	49.2	41.3	36.3	25.1	46.1
23	40.5	55.7	60.1	62.6	65.6	66.9	52.3	53.1	48.2	45.3	25.0	16.8	14.7	51.0	63.0	43.6	48.9	40.6	36.0	25.5	45.9
24	40.5	55.3	60.9	62.4	65.8	66.4	50.7	53.5	48.2	45.7	25.2	16.4	14.7	51.0	62.7	43.3	48.4	40.6	36.7	25.1	45.8
Mean	42.1	56.5	61.6	64.4	67.0	67.3	58.3	54.7	48.6	44.1	24.6	16.2	14.6	51.5	62.1	45.0	49.8	41.0	37.9	26.5	46.9
N	1	26	28	28	30	10	26	30	30	22	21	25	24	16	14	12	26	30	23	21	.....

excessive; otherwise, all incomplete days were omitted. Hourly values for the 443 complete days remaining were then corrected to standard air flow (10.0 liters per minute) and tabulated in units of micrograms per cubic meter (Γ), following the computational procedure given in Regener [9]. The flow rate is measured at the pump exhaust after circulation of the air through the device.

Annual ozone variation—Table 2, in addition to showing the mean daily values of surface ozone for each day of record, also gives the mean monthly value of surface ozone concentration for each month of the IGY during which observations were made. These monthly means are presented in graphical form for each individual month in figure 4, and for the combined 1957–58 data in figure 5. The February-March minimum is followed by a rapid rise in April to maximum concentrations in early winter, with only a gradual decrease through the late winter and spring and a sharp decrease during the summer.

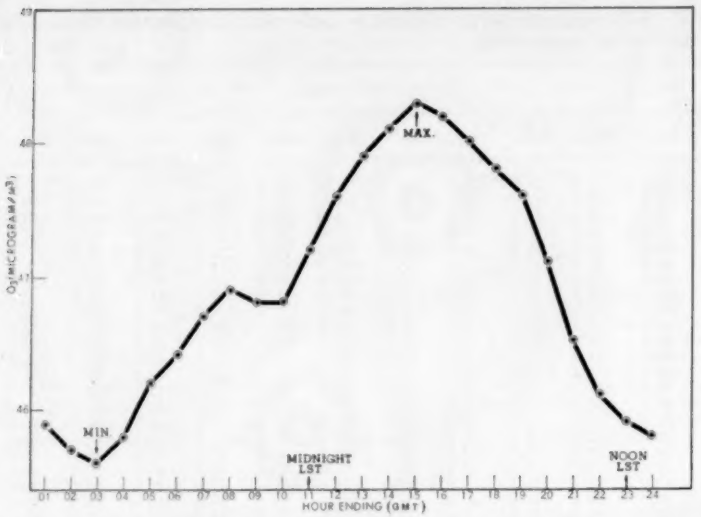

FIGURE 6.—Little America Station mean hourly surface ozone values, total period of record, 1957–58.

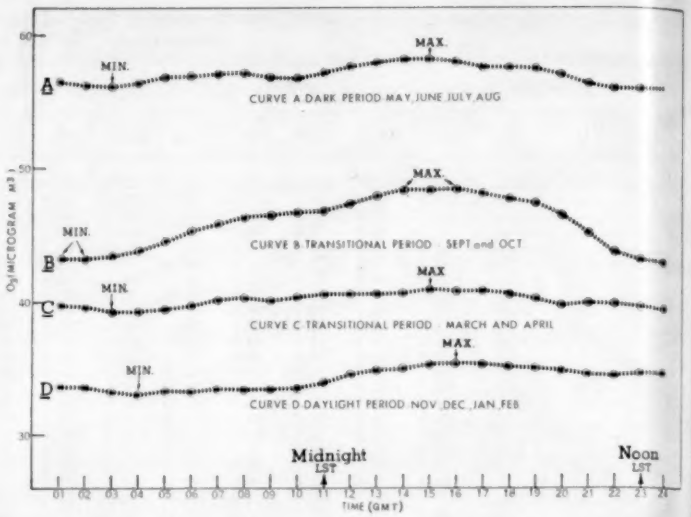
MAX.
MIN.
CURVE A DARK PERIOD MAY JUNE JULY AUG
CURVE B TRANSITIONAL PERIOD SEPT and OCT
CURVE C TRANSITIONAL PERIOD MARCH AND APRIL
CURVE D DAYLIGHT PERIOD NOV DEC JAN FEB
Midnight LST
Noon LST
TIME (GMT)

FIGURE 7.—Little America Station mean hourly surface ozone values by seasons, 1957–58 data.

Diurnal ozone variation—Table 3 shows the mean values of ozone concentration for each month by hour of the day, with values in micrograms per cubic meter and time in Greenwich, 11 hours later than standard time at Little America. Figure 6 gives the mean hourly values for all of the observations, while figure 7 depicts the mean hourly values by season as labeled. The curve in figure 6 shows a maximum at 0400 LST, and a minimum 12 hours later at 1600 LST. Although all of the seasonal curves plotted show the same general pattern, the daily variation is most regular and has the largest amplitude in the spring months of September and October.

The daily variation of surface ozone concentrations at mid-latitude plains stations has been found to vary in a manner which suggests a strong relationship to atmospheric thermal stability. During the day, peak ozone concentrations usually occur during the afternoon, while the minimum concentrations are found during the late evening or early morning hours. It has been suggested that the physical mechanism which causes the variation is due to an imbalance between the rate of ozone destruction at the earth's surface and the resupply processes from the higher tropospheric layers. The increased stability associated with the nighttime formation of a surface radiative inversion reduces the downward transport of ozone to the value where the rate of destruction exceeds the resupply; therefore, during the night, surface concentrations may approach zero. The relatively greater afternoon concentrations are attributed to the greater downward transport associated with instability mixing.

At mountain stations the daily surface ozone variation is usually found to be very small (Bowen and Regener [1]). However, recent results from studies made near the summit of Mauna Loa (Price and Pales [8]) have indicated that daily surface ozone variations may be strongly influenced by local mountain-valley wind circulations.

The terrain and the low-level atmospheric thermal structure found at Little America differ markedly from the mid-latitude environments where the majority of surface ozone measurements have been made. The absence of any vegetation and the extremely low atmospheric turbidity may result in lower ozone destruction rates. The low-level atmospheric thermal structure is dominated by a strong surface inversion which exists almost continuously except during the summer months when it may disappear completely or exist weakly as an isothermal layer. The above factors as well as the total absence or continuous presence of the sun would be expected to cause the amplitude of the diurnal ozone variation to be very small.

In order to investigate the magnitude and phase of the daily ozone oscillations, the data were examined by means of harmonic analysis. The results, which may be

TABLE 4.—*Harmonic constants for surface ozone diurnal and semidiurnal variations at Little America V, Antarctica*

Month	Year	A_1 micrograms per m.³	$A_1/\overline{O}_3$ percent	t_1 hr. after midnight (165° W.)	A_2 micrograms per m.³	$A_2/\overline{O}_3$ percent	t_2 hr. after midnight (165° W.)
January	1958	0.20	0.8	15.7	0.13	0.5	11.5
February	1958	1.45	9.0	6.2	.33	2.0	4.7
March	1958	.60	4.1	7.1	.15	1.0	.3
April	1957, 1958	.83	1.5	1.6	.05	.1	5.7
May	1957, 1958	.77	1.2	5.4	.97	1.6	4.8
June	1957, 1958	1.21	2.2	22.9	.90	1.6	3.9
July	1957, 1958	1.10	1.9	1.1	.18	.3	6.9
August	1957, 1958	.90	1.7	3.7	.19	.4	4.3
September	1957, 1958	3.75	7.8	1.9	.77	1.6	6.2
October	1957, 1958	1.12	2.8	1.9	.72	1.8	4.9
November	1957	1.19	2.5	4.5	.17	.3	5.1
December	1957	1.72	3.9	5.2	.65	1.5	.3

A_1=amplitude of diurnal oscillation; A_2 amplitude of semidiurnal variation.
$\frac{A_1}{\overline{O}_3}, \frac{A_2}{\overline{O}_3}$=Relative amplitude where $\overline{O}_3$ is mean monthly ozone concentration.
t_1=Time at which diurnal oscillation reaches its maximum value (A_1).
t_2=Time at which semidiurnal oscillation reaches its maximum value (A_2).

subject to errors due to the short period of record, are presented in table 4.

As anticipated the amplitudes are quite small. In general the diurnal variations are greater than the semidiurnal; however, during May the semidiurnal amplitude exceeds the diurnal. Since the thermal stability variation is greater in the summer than in the winter, one might predict that the relative amplitudes should be greater in the former season than in the latter. The data verify this prediction as the relative diurnal amplitudes average 4.6 percent for the summer months (December-January-February) and 1.9 percent for the winter months (June-July-August). The semidiurnal averages, although smaller, show an average relative amplitude 1.6 times greater in the summer than in winter.

The phase of the ozone diurnal oscillation exhibits a rather large variation which may be due to the short period of record. However, the time of the maximum usually occurs during the early morning hours. The early morning maximum tends to indicate that factors other than thermal stability variation may also be very important in determining the phase and amplitude of the diurnal ozone variation in polar regions.

Since the camp was on a 24-hour-a-day work basis, and since most or all of the camp contaminants consisted of smoke from heating stoves in 24-hour operation, there does not appear to be a diurnal cycle of camp contamination which could account for the phase of the observed diurnal variation of ozone concentration.

One possible factor which might influence the diurnal ozone variation is the daily worldwide pressure oscillation. The mass convergence associated with this pressure wave may cause an increase in the ozone density. In order to determine whether such a relationship exists, a harmonic analysis was made on all the available surface-pressure data obtained at the present and previous Little America sites. It is well known that the diurnal pressure variation is influenced by local weather and topography which complicate its worldwide characteristics. The semidiurnal variation, however, is worldwide and is the more important oscillation, especially in the polar regions. This fact is shown quite well by the harmonic constants for pressure in table 5. The semidiurnal wave exhibits greater uniformity in phase angle and amplitude than does the diurnal wave.

TABLE 5.—*Harmonic constants for surface pressure diurnal and semidiurnal variations at Little America sites, Antarctica*

Month	Year 19—	A_1 (mb.)	t_1 hr. after midnight (165° W.)	A_2 (mb.)	t_2 hr. after midnight (165° W.)
January	29, 30, 35, 41, 58	0.00	----------	0.10	1.5
February	29, 34, 40, 58	.00	----------	.10	10.2
March	29, 34, 40, 57, 58	.10	10.2	.10	10.7
April	29, 34, 40, 57, 58	.07	1.7	.10	10.5
May	29, 34, 40, 57, 58	.17	15.4	.10	10.4
June	29, 34, 40, 57, 58	.10	13.8	.17	9.5
July	29, 34, 40, 57, 58	.10	16.7	.14	.0
August	29, 34, 40, 57, 58	.14	15.7	.07	10.5
September	29, 34, 40, 57, 58	.27	15.9	.10	11.9
October	29, 34, 40, 57, 58	.00	----------	.14	11.3
November	29, 34, 40, 57	.10	7.9	.17	9.4
December	29, 34, 40, 57	.03	22.2	.03	10.6

A_1=Amplitude of diurnal pressure oscillation.
A_2=Amplitude semidiurnal pressure oscillation.
t_1=Time of occurrence of A_1.
t_2=Time of occurrence of A_2.

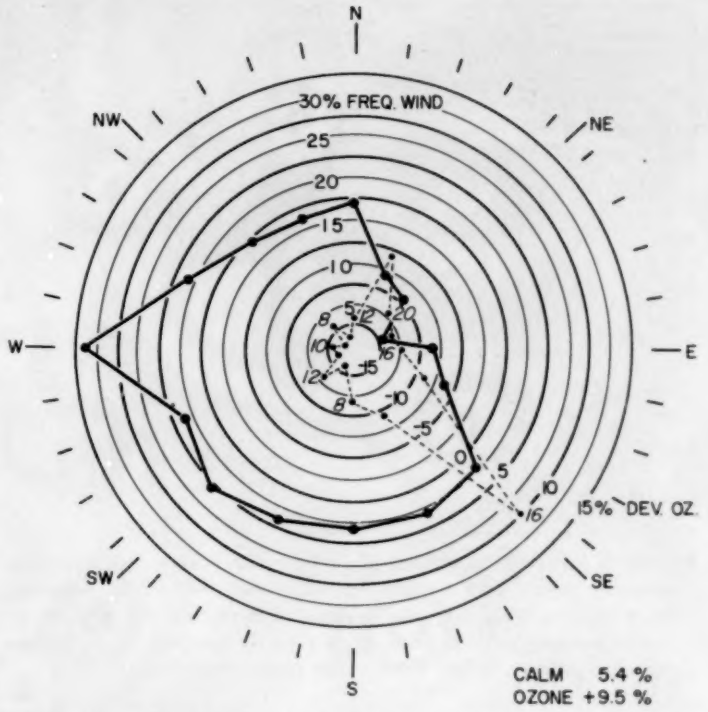

FIGURE 8.—Surface ozone and wind rose, Little America Station, June 1957 (from [4]). Heavy line connects values of percent deviation of surface ozone from monthly average for the various compass points. Dashed line connects percent frequency of occurrence of wind from the various directions. Numerals beside plotted wind points are average wind speed in knots.

A comparison of the harmonic constants for pressure with those for ozone indicates that there is little or no relationship between them. Therefore, from these limited data, it appears that the periodic daily pressure variation has little influence on the diurnal ozone oscillation.

Ozone and wind rose—Wind and ozone roses were constructed for selected months to show both the relative frequency of the different wind directions and the variation in surface ozone concentration with wind direction. This was done by plotting for each compass direction the percentage of time in the month during which the wind blew from that direction, based on the hourly surface wind observations; the mean value of surface ozone hourly readings for those hours when the wind blew from a specified direction was computed, and the result plotted as a percentage deviation from the overall mean monthly ozone value.

The June 1957 Little America rose (fig. 8) shows positive deviation of ozone amounts with westerly and calm winds, and negative deviation with easterly winds. In August 1958, the computations show very broadly the same general pattern although the rose is more irregular and

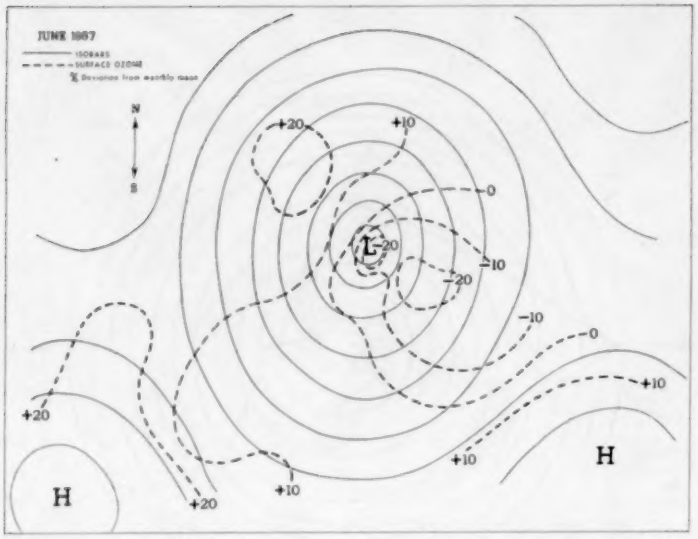

FIGURE 9.—Percent deviation of surface ozone concentration from monthly mean, and sea level pressure pattern, Little America, June 1957. Each value for percent of deviation was plotted on model pressure pattern at position of Little America in the surface pressure pattern at the time of the ozone observation.

the calm wind deviation is negative. February 1958 shows positive deviations with all wind directions from WSW through N to NE, while with calm winds and most of the other wind directions there are negative deviations. All of these months show a net transport of both air and ozone from the continent northward to the ocean.

Relation with sea level pressure field—The relationship of surface ozone concentration to the sea level weather chart is illustrated in figure 9. Charts similar to the one for June 1957 shown here were prepared for each month April through September 1957 by plotting the deviation of the ozone concentration at 0000, 0600, 1200, and 1800 GMT from the mean monthly concentration. Each value was plotted in the model pressure pattern by determining the position of Little America with respect to the surface weather pattern at the time of the observation. The 6-hourly synoptic maps prepared at the IGY Antarctic Weather Central were utilized in determining the relationship.

The surface ozone pattern depicted by the June 1957 chart is typical of all the charts. In general, the lower values were found to occur in the southeast quadrant of the surface Low. Cyclones entering the Ross Sea usually approach Little America from the northwest. These negative deviations may be the result of the advection of air with lower ozone concentrations from off the ocean. Positive deviations were located in the northwest quadrant of the Low and in the cold anticyclone occasionally found over the Ross Sea. The advection of ozone-rich air from the continent into the rear of the cyclone may account for the maximum observed there. The positive deviations found in the high pressure regions may be the result of the downward transport of ozone by subsidence processes usually associated with a polar anticyclone.

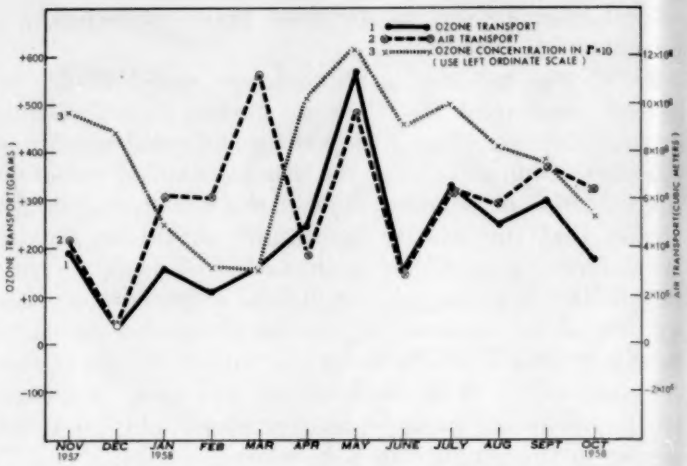

FIGURE 10.—Little America Station mean monthly surface ozone and meridional mass transport of air and ozone.

Ozone transport—Table 6 shows the monthly values of volume transport of air and mass transport of ozone along the meridian at Little America. These values were obtained as follows: the net meridional component of wind for each day was computed from the 24 hourly wind observations and multiplied by the average ozone concentration for that day to give daily ozone mass transport; these were then summed algebraically to give the total monthly and finally annual transport. In this case, when daily values for ozone concentration were missing, linearly interpolated values were used (parenthetical values in table 2). Units for air transport for the month are 10^6 m.^{3} of air through an area of 1 m.^{2} normal to the meridian at anemometer height (about 10 m.). For the monthly ozone transports the units are grams of ozone through an area of 1 m.^{2} at anemometer height, assuming that the ozone concentration is the same at intake height and anemometer height. Each month shows a northward (positive) component of the air transport with a minimum in December and maxima in March and May. The ozone transport northward shows a minimum in December and a maximum in May (the low March ozone value outweighs the high air transport). In figure 10 are presented graphs of the meridional mass transport of ozone, the meridional volume transport of air, and the mean monthly surface ozone values, the latter taken from figure 4.

TABLE 6.—*Meridional air and ozone transports at Little America*

Month	Net meridional air transport (10^6 m.^{3}/m.^{2})	Net ozone transport (gm./m.^{2})
November 1957	+4.399	+198.4
December 1957	+.682	+33.6
January 1958	+6.172	+156.4
February 1958	+6.070	+107.8
March 1958	+11.288	+163.1
April 1958	+3.781	+242.2
May 1958	+9.667	+567.3
June 1958	+2.973	+146.5
July 1958	+6.351	+324.7
August 1958	+5.802	+247.9
September 1958	+7.445	+297.2
October 1958	+6.305	+171.2
12 months	+70.935	+2652.3

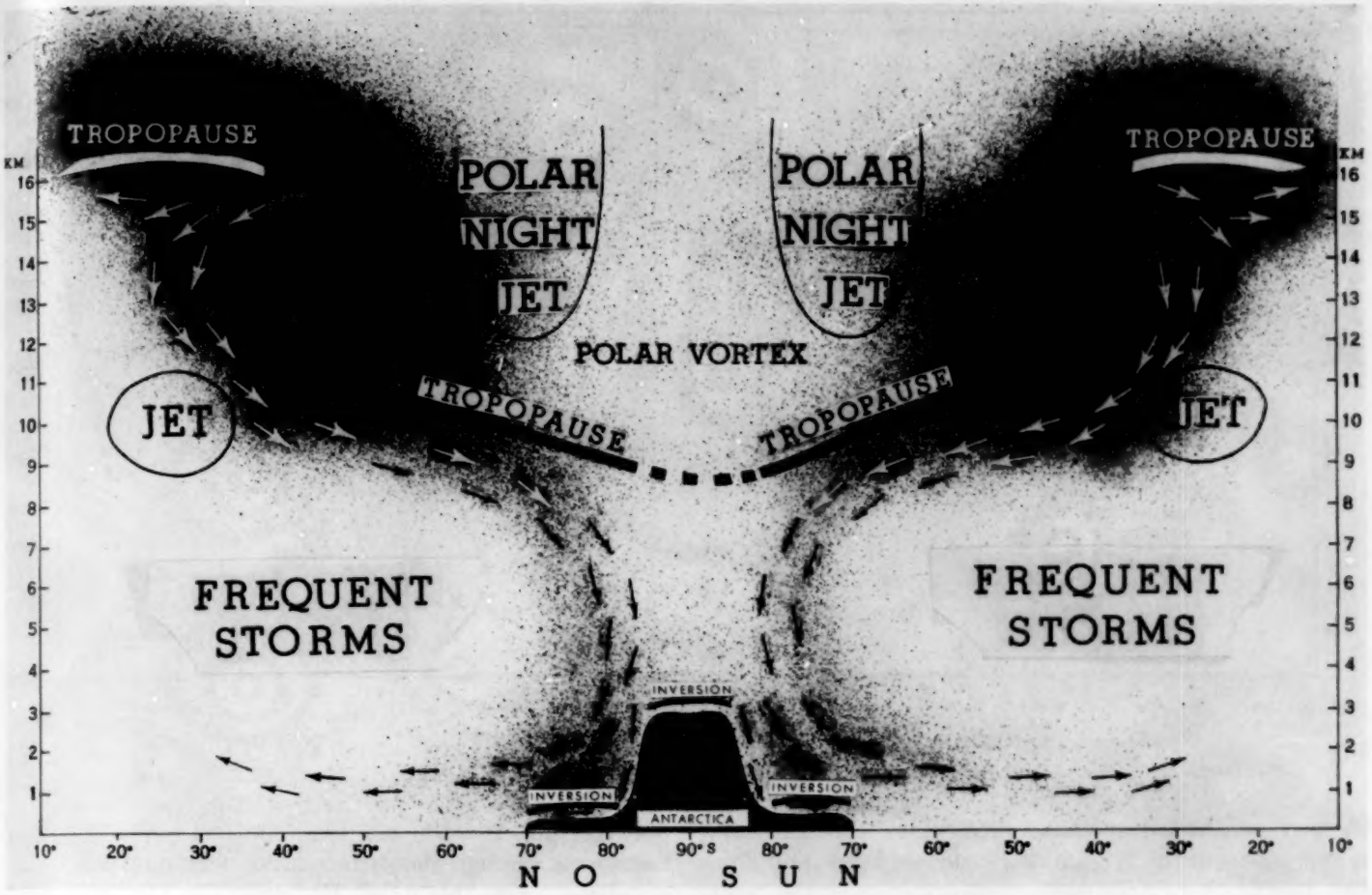

FIGURE 11.—Schematic representation of winter ozone cycle in Antarctica.

5. POLAR-NIGHT OZONE BUDGET AND CIRCULATION

Referring to figure 4 we see that during 4 months of the dark period, June through September 1958, the surface ozone content was fairly constant at 38 to 50 micrograms $m.^{-3}$. During this same 4-month period the net ozone flow northward from Little America was 1016 gm. $m.^{-2}$ (see table 6 and fig. 10). If there is to be a steady state then as much ozone must flow in as flows out, since we assume no ozone is created or destroyed by photochemical or other means.

The ozone influx can occur in the stratosphere or in the troposphere. Since ozone is usually found in greatest amount in the lower stratosphere one would expect that this layer would be the most likely source of supply of ozone to the surface air over Antarctica. However, there are two difficulties facing this explanation. First, the strong winter circumpolar jet stream in the low stratosphere (Moreland [7]) would discourage significant transport of ozone into the interior of the Antarctic continent (Wexler [13]). Second, even if there were a significant stratospheric influx of ozone into the interior, it would require many days of radiative cooling over the continent for this air to sink through the stable stratosphere, then through the tropopause into the troposphere, and to descend into and flow out with the surface layer of air. For example, on August 6, 1957, a day of coldest stratosphere at the South Pole (−91° C. at 50 mb.), the potential temperature at 100 mb. was 360° A.; at the top of the surface inversion (555 mb.) it was 286° A., and at the surface (702 mb.) it was 255° A. Even a large cooling rate of 5° C. day^{-1} would require the same air to remain over Antarctica for more than 20 days in order to reach the surface, an unlikely event. Of course, turbulent transport downward would occur, but in view of the strong stability of the stratosphere and surface layer, this would be a slow process too.

It thus appears that the major influx of ozone into Antarctica occurs in the troposphere above the surface layer. The winds responsible for this transport are associated with the vigorous winter storms which move around and into the continent, transporting such vast quantities of real and latent heat that tropospheric temperatures show very little decline during the dark period, April to September (Wexler [13]). In addition to real heat and water vapor these same large eddies can also transport into Antarctica ozone from lower latitudes. This ozone, which is manufactured photochemically in the sunlit stratosphere, probably enters the troposphere through the tropopause gap associated with the mid-latitude (30°–35° lat.) jet stream. (See fig. 11.) It is then caught in the undulating westerly current, and makes

545014—60——2

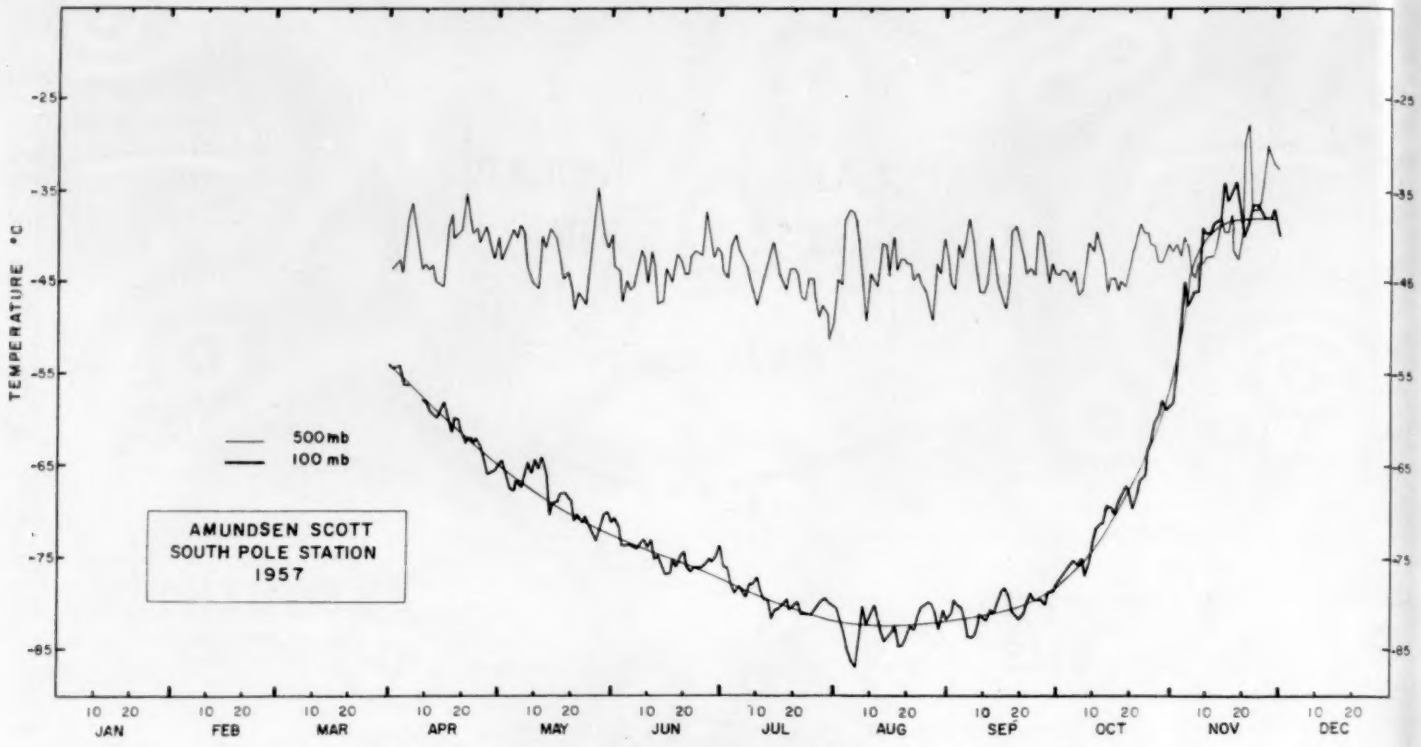

FIGURE 12.—Daily temperatures and seasonal trend, 500 mb. and 100 mb., South Pole, 1957.

its way southward to Antarctica where the air sinks, becomes part of the 2–3-km. thick surface layer, and flows northward. Very little ozone is shown crossing the polar-night jet into the center of the stratospheric polar vortex.

If the principal influx of ozone into Antarctica occurs in the middle and upper troposphere, what concentration of ozone is required? We can compute this roughly in two ways: assume a fictitious Antarctic continent bounded by the 72° S. latitude circle (area 12.5×10^6 km.^{2} compared to the actual 13.5×10^6 km.^{2}). Because of lack of information elsewhere on the Antarctic coast we shall assume first that the Little America mean monthly ozone transport applies to the entire coast. At Little America the 1000–700-mb. layer (which extends from sea level to 2.5 km.) is the layer of outflow in June, July, and August (Court [2], p. 69). If we assume that the surface ozone transport is constant through this layer, this first model results in a northward flow of 31.8×10^{12} gm. of ozone during June–September 1958.

Since, however, the ozone flow across the coast depends on the mass movement of air across the coast, a second computation was made based on values for the entire coast worked out by Rubin [10] for June and December 1958, while in residence at the Soviet IGY Station, Mirny. Later, on his return to Washington where the original U.S.-Antarctic radiosonde observations were available, Rubin corrected these values slightly and completed the computations for the period June through December 1958. These were calculated for tropospheric layers 850–700 mb., 700–500 mb., and 500–300 mb. The mass transports through the surface layer, 850–1000 mb. (near sea level) were obtained by extrapolating downward Rubin's monthly values. In this computation the ozone mixing ratio observed at Little America was assumed for the entire Antarctic coast, taken as the 72° S. latitude circle.

Based on these assumptions and the Little America observations we find that during the 4-month period, June–September 1958, when the surface ozone concentration at Little America was fairly constant at 38 to 50 micrograms m.$^{-3}$, the total ozone *outflow* across the Antarctic coast was 72.8×10^{12} gm., or a little more than twice the transport computed by the first simple model. We shall use the larger transport figure to see if the required ozone concentration in the inflow layer 700 to 300 mb. is a reasonable value. During this same period the air *inflow* in the layer 700 to 300 mb. (2.5 km. to 8 km., the tropopause) was 26.7×10^{20} gm. Thus the ozone concentration in this upper tropospheric layer required to maintain a steady state was 2.72×10^{-8} gm. ozone (gm. air)$^{-1}$ or 1.64 parts per hundred million (pphm) by volume. This concentration compares quite well with the average value in the 700–300-mb. layer observed by ozonesondes at Halley Bay, Antarctica (75°31′ S., 26°36′ W.) on January 24 and July 3, 1958 (MacDowall [6]).

Thus, it appears that tropospheric advection of ozone can by itself account for the high values of surface ozone

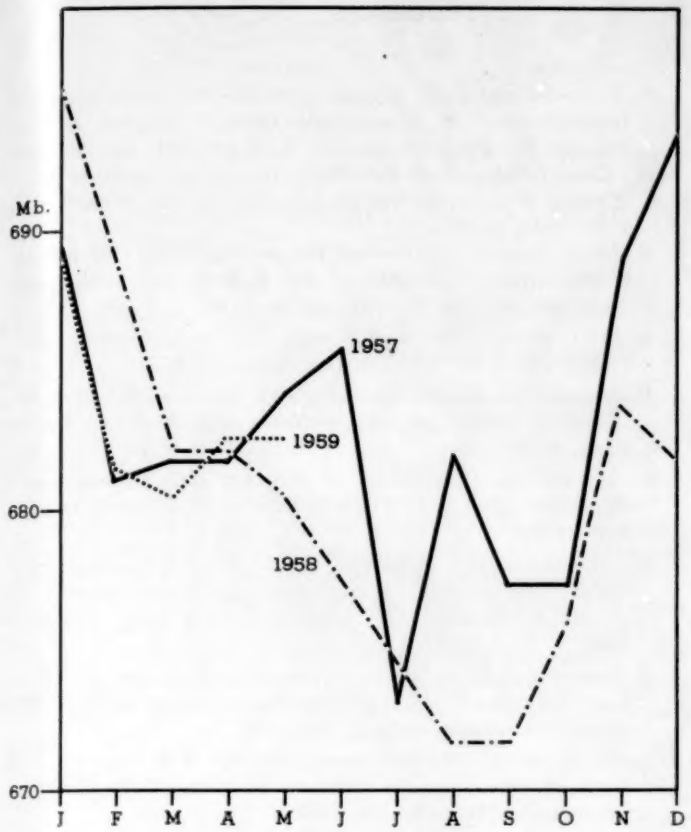

FIGURE 13.—Average monthly surface pressure, South Pole.

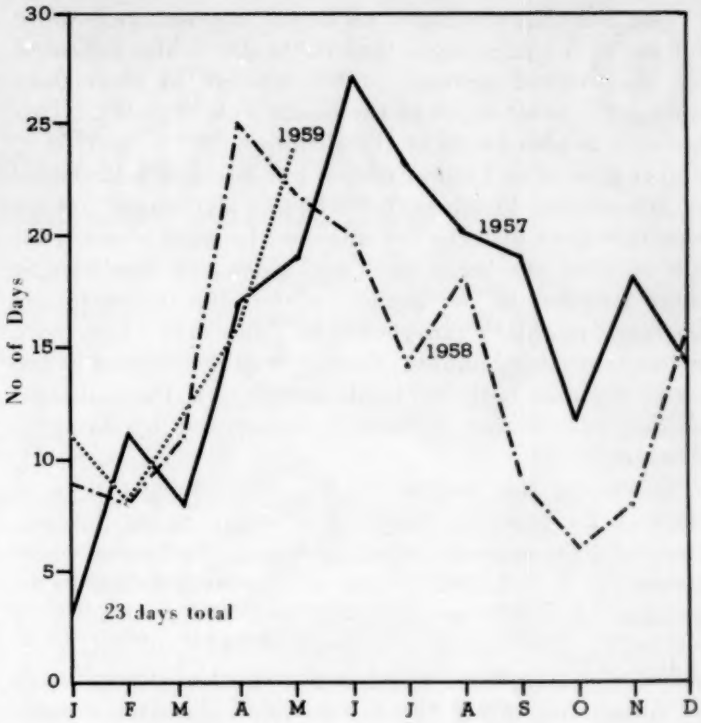

FIGURE 14.—Number of clear days, by months, South Pole. Observations were made on only 23 days in January 1957.

without calling on contributions from the stratosphere over Antarctica. Even the large increase from 15 micrograms m.$^{-3}$ in March to 62 in May 1958 can be accounted for by the inward advection of tropospheric air containing observed concentrations of ozone.

The figures in table 6 require an average of 250×10^{12} gm. sec.$^{-1}$ of air leaving Antarctica in the 0–2.5-km. layer from June–September, and 252×10^{12} gm. sec.$^{-1}$ of air entering Antarctica, or seemingly a near balance. However, even an imbalance of 2×10^{12} gm. sec.$^{-1}$ would still result in an increase in average surface pressure by over 100 mb. in 4 months; the transport figures are not accurate enough to determine precisely the small difference between the two large numbers—inflow and outflow. Nevertheless, changes in monthly mean pressures at interior stations in Antarctica generally agreed in sign with the preliminary estimates of mass advection across the Antarctic coast for May–July and November–December 1958, despite the fact that possible stratospheric influences were neglected (Rubin [10]).

To complete the air mass cycle, descent of air over Antarctica is required with an average downward velocity of about 2 km. day^{-1}. For the temperature lapse rates observed in the mid-troposphere over Antarctica this means a cooling of about 5° C. day^{-1} *if* the tropospheric temperatures are to remain essentially constant from day to day. This cooling must be done by radiative losses and is too high by a factor of 2 compared to cooling rates observed at the South Pole station and at the Hallett Station (72°18′ S., 170°18′ E.) during April–June 1959. The balloon-borne radiometer developed by Suomi et al. [11] was used for this measurement and fuller results will be published later. If the cooling rate is not large enough to permit sinking of air at the required steady-state rate then local heating must result. The large day-to-day fluctuations of temperature at 500 mb. during the 1957 winter at the South Pole (fig. 12) (Moreland [7]) show that the temperatures are not "essentially constant," but whether these fluctuations are caused primarily by variations in advection or by variations in sinking and cooling rates is still to be determined.

During the remaining 3 months for which the preliminary advective rates are available, i.e., October, November, and December, there was an outward flow of 308×10^{12} gm. sec.$^{-1}$ in the 1000–700-mb. layer and an average inward flow of 350×10^{12} gm. sec.$^{-1}$ in the 700–300-mb. layer, seemingly a larger imbalance than in the June–September period. The presence of solar radiation in October–December should decrease the free air radiative cooling rates and thus decrease the compensating downward velocities. This should cause air to accumulate in the troposphere and thus should increase the surface pressure. As may be seen in figure 13, the South Pole station pressures are larger in summer than in winter by about 10 mb., in agreement with the above reasoning.

The fact that sinking of air in the troposphere is more intense in the polar night than in the day is also indicated by the marked increase in the number of clear days during the polar night at the South Pole (fig. 14). This increase is also found at Byrd Station (80° S., 120° W.), and is present at Little America but less distinct because of the coastal location and influence of storms. Since cloudless days with the sky obscured by wind-blown snow are counted as cloudy days and since this condition is more frequent in the windier winter, the contrast may be more marked than shown in figure 14. The more vigorous sinking motions in winter would tend to dissolve cloud systems both by local warming (if the radiative cooling rate is not sufficiently large) and by bringing down drier air.

In closing this section on the ozone budget it is of interest to examine briefly the water vapor budget. Loewe [5] has estimated that the transport of water vapor across 71° S. is 1.35×10^{18} gm. yr.$^{-1}$ corresponding to an average of liquid precipitation over Antarctica of 10 cm. yr.$^{-1}$. This means an average of 0.45×10^{11} gm. sec.$^{-1}$ inflow of water vapor which is deposited as precipitation in Antarctica during the 4 months of the dark season, June–September, when the average inflow of air is 2.5×10^{14} gm. sec.$^{-1}$. Thus, the mixing ratio of the precipitated water vapor is 0.18×10^{-3} gm. gm.$^{-1}$ or 0.18 gm. kg.$^{-1}$.

This value can be compared with the precipitable water content of the air column from 700 to 300 mb. over Hallett Station taken as typical of air entering Antarctica, minus that over the South Pole taken as typical of the air after precipitation has occurred. For the period, June–September 1958, this difference, expressed in gm. kg.$^{-1}$ of the air mass above 700 mb., is 0.10 gm. kg.$^{-1}$ which is smaller than the presumed winter precipitated amount, 0.18 gm. kg.$^{-1}$. It is probable that this latter figure is too large since the winter precipitation is small compared to the other seasons.

REFERENCES

1. G. I. Bowen and V. H. Regener, "On the Automatic Chemical Determination of Atmospheric Ozone," *Journal of Geophysical Research*, vol. 56, No. 3, Sept. 1951, pp. 307–324.
2. A. Court, "Meteorological Data for Little America III," *Monthly Weather Review, Supplement* No. 48, Washington, D.C., 1949, 150 pp.
3. G. M. B. Dobson, "Observers' Handbook for the Ozone Spectrophotometer," *Annals of the International Geophysical Year*, vol. V, Part I, 1957, pp. 46–114.
4. S. Fritz, et al., "Status of Special Studies in Meteorology," *IGY Bulletin* No. 20, February 1959, pp. 1–7.
5. F. Loewe, "Études de Glaciologie en Terre Adélie 1951–52" *Actualites Scientifique et Industrielles* 1247, Hermann & Cie., Paris, 1956.
6. J. MacDowall, "Soundings of the Antarctic Ozonosphere", Paper presented at IUGG/WMO Ozone Symposium, Oxford, July 1959.
7. W. B. Moreland, "Antarctic Stratosphere Circulation and Ozone Observations," Paper presented at Symposium on Antarctic Meteorology, Melbourne, Australia, February 1959 (to be published).
8. S. Price and J. Pales, "Some Observations of Ozone at Mauna Loa Observatory, Hawaii," Paper presented at IUGG/WMO Ozone Symposium, Oxford, July 1959.
9. V. H. Regener, *Automatic Ozone Recorder*, The University of New Mexico, Dept. of Physics, Technical Manual, Albuquerque, N. Mex., Oct. 30, 1956.
10. M. Rubin, "Advection Across the Antarctic Boundary," Paper presented at Symposium on Antarctic Meteorology, Melbourne, Australia, February 1959 (to be published).
11. V. E. Suomi, P. M. Kuhn, and D. O. Staley, "Direct Measurement of Infrared Radiation Divergence to 160 Millibars," *Quarterly Journal of the Royal Meteorological Society*, vol. 84, No. 360, April 1958, pp. 134–141.
12. E. Vigroux, "Contributions a l'Étude Expérimentale de l'Absorption de l'Ozone," *Annales de Physique*, N. 8, Sept./Oct. 1953, pp. 709–762.
13. H. Wexler, "The 'Kernlose' Winter in Antarctica," *Geophysica*, vol. 6, Nos. 3–4, 1959, pp. 577–595.

ON CHANGES IN ZONAL MOMENTUM IN SHORT-RANGE NUMERICAL PREDICTION

A. WIIN-NIELSEN, Air Weather Service, U.S. Air Force

Joint Numerical Weather Prediction Unit, National Meteorological Center, Suitland, Md.

[Manuscript received December 29, 1959; revised February 19, 1960]

ABSTRACT

Different factors influencing the changes in the zonally averaged wind are investigated. It is evident from recent investigations of errors in the zonally averaged winds in the non-divergent, one-parameter model that the convergence of the meridional transport of zonal momentum concentrates too much momentum in the middle latitudes and predicts too small amounts of momentum in the low and high latitudes.

The other factors influencing the changes of zonal momentum, i.e., mean meridional circulations, friction, and vertical transport of momentum, are investigated on an averaged basis in the following sections: In section 3 it is shown that the divergent, one-parameter model will reduce the errors in zonal momentum predicted by the non-divergent model, due to an implied mean meridional circulation. The corrections to the predictions of changes in zonal momentum caused by mean meridional circulations in a two-parameter model are investigated in section 4 by the aid of operationally computed initial values of the vertical velocities. It is shown that reductions in the errors of the non-divergent model with respect to zonal momentum can be expected with a careful arrangement of the information levels in a two-parameter model.

Section 5 contains a similar investigation of the averaged contribution of vertical advection to changes in zonal momentum. It is found that this contribution is smaller than the one resulting from mean meridional circulations, and further that the contribution from the vertical advection of momentum is not likely to reduce the errors found in the non-divergent predictions.

The main conclusion from the study is that the contributions from mean meridional circulations and surface friction are the most important for the reductions of errors in the prediction of zonal momentum in the non-divergent model. Some reduction of the errors can be expected in the divergent, one-parameter model or in a two-parameter model with a proper arrangement of the information levels. In order to incorporate surface friction in a realistic way, and further in order to avoid the artificial constraint of a non-divergent level appearing in a two-parameter model, it is most likely that more than two parameters are needed for accurate forecasts of zonal momentum.

1. INTRODUCTION

The expansion of the area used in operational numerical predictions has shown a number of problems connected with forecasts of the very large-scale features of the flow in the atmosphere. The problems connected with forecasts of the motion of the planetary waves have been treated in earlier investigations by Wolff [13], Cressman [3], and the author [11]. Another problem is connected with the prediction of the zonally-averaged flow; i.e., the mean zonal wind.

The errors in the zonal winds as predicted by the non-divergent barotropic model have recently been investigated in a very instructive manner by Bristor [1] who shows that the error pattern taken daily or in the average over a month has a very systematic distribution with latitude. By and large, the errors may be characterized by saying that the non-divergent barotropic model predicts too weak averaged zonal winds in the very low and the very high latitudes and too strong mean zonal winds in the middle latitudes. The error pattern is persistent month after month in the period analyzed by Bristor [1] and he suggests that the cause of these errors is the lack of momentum sources and sinks in the barotropic model.

If the 500-mb. flow is considered as a representation of the vertically averaged flow of the atmosphere, it follows, as shown for instance in [1], that surface friction is the only source of momentum which can influence the rate of change of the zonal wind apart from the effect of the convergence of the meridional transport of zonal momentum. The latter effect is, however, incorporated in the barotropic model. In this formulation we could therefore ascribe the errors in the predicted 500-mb. mean zonal winds to the neglect of the effects caused by surface friction.

On the other hand, if we consider the 500-mb. flow as a divergent flow, we may get changes in the mean zonal winds caused by the effects of the Coriolis term in the equations of motion, or in other words by the effects of a mean meridional circulation. In experiments on the general circulation of the atmosphere, Phillips [8] showed that

the effects of the mean meridional circulation very nearly balance the effects of surface friction at the lower level (750 mb.), while the mean meridional circulation at the upper level acts opposite to the effects of the meridional transport of momentum at the upper level (250 mb.). The effects of the mean meridional circulation in a two-parameter model are therefore to decrease the mean zonal wind in the middle-latitudes at the upper level and to increase the wind at the lower level.

In view of these results it seems that we have two equally important factors in the lower troposphere and one in the higher troposphere to change the forecasts, which would be produced considering only the horizontal part of the motion. It also appears that these two factors, friction and mean meridional circulation, must be considered together because they act in opposite directions in the lower part of the atmosphere. If we use only two parameters to represent the vertical structure of the atmosphere, there will always be a level in the model where the effects of the mean meridional circulation vanish, the so-called non-divergent level. It seems very important to place this level as close as possible to the actual position of the corresponding level in the atmosphere, because otherwise we will ascribe errors, which appear in the model, solely to surface friction effects, although they actually could be caused by vertical velocities not included in the model.

It is obvious that great errors in the prediction of mean zonal winds can have a marked influence on the disturbances and their motion. From data in [1] one sees that an error of about 10 knots in 72 hours appears even on the monthly average for January and February 1958. If we for a moment assume that disturbances move approximately with the wind speed and that a mean error of 5 knots exists during a 72-hour period, it means that troughs and ridges are displaced about 650 km. too much to the east in the middle latitudes and a similar amount too far toward the west in the low latitudes. The result is that the troughs and ridges get a greater positive tilt (SW-NE tilt), which means that still more momentum is transported into the middle latitudes causing a further error in the tilt. We are therefore here dealing with a type of systematic, accumulating error, which, if strong enough, will result in a greater and greater tilt of the systems.

A special aspect of such a systematic error comes up in connection with the objective analysis scheme [4]. The 12-hour barotropic forecasts are used as a first guess for a subsequent 500-mb. analysis. It may happen that a sufficient amount of data does not exist to remove the systematic error in the first guess completely, with the result that even the initial analysis for the next forecast contains too strong zonal winds in the middle latitudes and too weak zonal winds to the north and south of the middle latitudes. This effect has actually been noticed in a comparison made between analyses produced by the present objective analysis scheme and analyses prepared by conventional methods.

It is the purpose of the following sections to investigate the possibilities which we have to remove these systematic errors from the barotropic forecasts. We have two effects, which should be considered: The effects of mean meridional circulations and surface friction. In section 3 we show that the present divergent, one-parameter model tends to reduce the errors in the mean zonal wind obtained from a non-divergent, one-parameter model. Finally, we present an analysis of the vertical motions computed from a two-parameter model, which shows that we can expect an improvement in the prediction of zonally averaged winds with a proper choice of the non-divergent level.

2. GENERAL AND SIMPLIFIED PROGNOSTIC EQUATIONS FOR THE MEAN ZONAL FLOW

The first equation of motion may be written in the following momentum form in pressure coordinates:

$$\frac{\partial u}{\partial t}+\frac{\partial uu}{\partial x}+\frac{\partial uv}{\partial y}+\frac{\partial u\omega}{\partial p}=-\frac{\partial \phi}{\partial x}+fv. \tag{2.1}$$

u, v, and ω are here the three components of the velocity vector; $\phi=gz$ the geopotential; f the Coriolis parameter; g the acceleration of gravity. No assumptions are made regarding the velocity components which may contain divergent as well as non-divergent components.

We define the following averaging operator:

$$\overline{(\ )}=\frac{1}{L}\int_0^L (\ )\,dx \tag{2.2}$$

where L is the length of the latitude circle.

Applying (2.2) to (2.1) we obtain

$$\frac{\partial \bar{u}}{\partial t}+\frac{\partial \overline{uv}}{\partial y}+\frac{\partial \overline{u\omega}}{\partial p}=+f\bar{v}. \tag{2.3}$$

It should be noted that an equation quite similar to (2.3) can be obtained by averaging the vorticity equation in its complete form:

$$\frac{\partial \zeta}{\partial t}+\nabla\cdot(\eta\mathbf{V})+\frac{\partial}{\partial x}\left(\omega\frac{\partial v}{\partial p}\right)-\frac{\partial}{\partial y}\left(\omega\frac{\partial u}{\partial p}\right)=0. \tag{2.4}$$

We now obtain applying (2.2):

$$\frac{\partial}{\partial y}\left[\frac{\partial \bar{u}}{\partial t}+\frac{\partial \overline{uv}}{\partial y}+\frac{\partial \overline{u\omega}}{\partial p}-f\bar{v}\right]=0. \tag{2.5}$$

The last term on the left side of (2.3), the effect of vertical transport of momentum, is seldom incorporated in short-range prediction. We later present evidence that justifies the neglect of this term at least in two-parameter models. The neglect of the term corresponds to disregarding the vertical advection and the twisting term in the vorticity equation. If the flow further is assumed to be

strictly non-divergent and frictionless, we get the following simplified form of the momentum equation, which applies in a non-divergent, one-parameter model:

$$\frac{\partial}{\partial y}\left[\frac{\partial \bar{u}}{\partial t}+\frac{\partial \overline{uv}}{\partial y}\right]=0. \tag{2.6}$$

The term $\partial\overline{uv}/\partial y$ may of course in this case equally well be written $\overline{v\partial u/\partial y}$, because the second part

$$\overline{u\partial v/\partial y}=-\overline{\partial\left(\frac{1}{2}u^2\right)/\partial x}$$

vanishes identically.

A quasi-non-divergent model would apply a consistent form of the vorticity equation in the form (Wiin-Nielsen [10]):

$$\frac{\partial \zeta}{\partial t}+\mathbf{V}_\psi\cdot\nabla(\zeta+f)=-f_0\nabla\cdot\mathbf{V} \tag{2.7}$$

which would result in an equation for the rate of change of mean zonal wind of the form

$$\frac{\partial}{\partial y}\left(\frac{\partial \bar{u}}{\partial t}+\frac{\partial \overline{u_\psi v_\psi}}{\partial y}-f_0\bar{v}\right)=0 \tag{2.8}$$

which, compared with (2.5), would result in a correct form.

Using an inconsistent form of the vorticity equation

$$\frac{\partial \zeta}{\partial t}+\mathbf{V}_\psi\cdot\nabla(\zeta+f)=-\eta\nabla\cdot\mathbf{V} \tag{2.9}$$

where $\eta=\zeta+f$, f variable, would result in a zonal momentum equation as follows:

$$\frac{\partial}{\partial y}\left[\frac{\partial \bar{u}}{\partial t}+\frac{\partial \overline{u_\psi v_\psi}}{\partial y}-f\bar{v}\right]+\beta\bar{v}-\overline{\zeta\nabla\cdot\mathbf{V}}=0 \tag{2.10}$$

It is obvious from (2.10) that we may obtain fictitious changes in the zonal winds if the relative vorticity and the divergence are correlated along the latitude circles.

3. COMPARISON BETWEEN NON-DIVERGENT AND DIVERGENT ONE-PARAMETER MODELS

It has recently been found necessary to modify the non-divergent barotropic model in such a way that the motion of the ultra-long waves is greatly reduced. The modification is made by an estimate of the divergence term in the vorticity equation. The magnitude of the coefficient may be estimated in different ways. One way has been demonstrated by the author [11]. The argument for an introduction of a certain divergence in the one-parameter model has been the modification of the motion of the long waves. It is, however, obvious that we also by so doing change the prediction of the zonally-averaged winds, because we indirectly introduce a mean meridional circulation, which in turn has a certain effect on the zonally-averaged flow.

Considering the remarkable success of the divergent, one-parameter model in prediction of the 500-mb. flow pattern one gets the impression that this model in a fortunate way contains the essential features of the mid-tropospheric flow, at least with respect to the zonally-averaged changes predicted by the model. It is certainly true that the model does not have any mechanism which can predict rapid deepening or filling, because it does not include the effects of temperature advection, diabatic heating, and friction. Nevertheless, it will predict zonally-averaged changes, the results comparing favorably with predictions computed by models that contain these effects. The reason is of course that the effects, which have been disregarded, by and large compensate each other. We shall demonstrate this at the end of section 3.

The first purpose is to demonstrate that the long-wave modification also decreases the error in the zonal flow. Naturally, we could demonstrate this by a computation of forecasts with and without the long-wave modification, but in order to get a clear picture of the mechanism at work we shall consider a theoretical example.

We may picture the process which creates the error in the non-divergent forecast as follows. As a result of the positive tilt in the low latitudes we transport (too much) momentum into the middle latitudes. The negative tilt in the high latitudes in a similar way transports momentum into the middle latitudes. As this process, according to Bristor's [1] analysis of the errors, gives too great changes in the mean zonal winds, there must be some processes which counteract this effect.

In order to look into the effect of the divergence term in the present operational one-parameter model we shall consider an initial flow which has the characteristic tilts. Such a flow may be described by a perturbation stream function having the following form:

$$\psi(x,y)=A\cos\mu y\cos\kappa(x+\alpha y^2). \tag{3.1}$$

To simplify our computations we consider a rectangular region bounded to the north and south by walls and having an extension in the x-direction of one wavelength. The boundary conditions at the walls will be those given by Phillips [7]; i.e.

$$v=\frac{\partial\psi}{\partial x}=0 \text{ and } \frac{\partial}{\partial y}\left(\frac{\partial\bar{\psi}}{\partial t}\right)=0 \text{ at the walls.} \tag{3.2}$$

The arrangement of the coordinate system will be with the x-axis parallel to the walls and with the y-coordinate at the walls to be $y=\pm W$. With these definitions we have

$$\mu=\frac{\pi}{2W},\ \kappa=\frac{2\pi}{L} \tag{3.3}$$

where L is the wavelength in the x-direction. Now, the parameter α is related to the slope of the trough and ridge lines in the flow, these lines being defined by the condition

$v=0$. From the expression for ψ it is seen that the trough and ridge lines are curves described by the equation

$$x+\alpha y^2=0 \tag{3.4}$$

The curves are parabolas which for $\alpha>0$ are open toward the "west"; i.e., with a positive tilt in the lower half and a negative tilt in the upper half. It is also seen that the smaller α is, the smaller will be the tilt. The factor cos μy means that we assume a maximum disturbance amplitude in the middle of the channel and further that the boundary condition $v=0$, $y=\pm W$ is automatically satisfied.

The problem is now to predict the tendency in the mean zonal wind speed for the initial flow pattern. The vorticity equation applying to the divergent, one-parameter model has been discussed at length by the author [11]. The final form of the prognostic equation may be written:

$$\frac{\partial \zeta}{\partial t}-r^2\frac{\partial \psi}{\partial t}=J(\nabla^2\psi+f,\psi) \tag{3.5}$$

which averaged along the latitudes reduces to

$$\frac{d^2}{dy^2}\left(\frac{\partial \bar{\psi}}{\partial t}\right)-r^2\left(\frac{\partial \bar{\psi}}{\partial t}\right)=\frac{\partial^2(\overline{uv})}{\partial y^2}=\frac{\partial^2(\overline{u'v'})}{\partial y^2} \tag{3.6}$$

where u' and v' are the perturbation velocities. It is easily seen that

$$\overline{uv}=\overline{u'v'}, \text{ because } \bar{v}=\frac{\overline{\partial \psi}}{\partial x}\equiv 0$$

With the expression (3.1) for the perturbation stream function (3.6) becomes

$$\frac{d^2}{dy^2}\left(\frac{\partial \bar{\psi}}{\partial t}\right)-r^2\left(\frac{\partial \bar{\psi}}{\partial t}\right)=D\sin(2\mu y)+Ey\cos(2\mu y) \tag{3.7}$$

where

$$\begin{cases} D=2\alpha\mu\kappa^2A^2 \\ E=2\alpha\mu^2\kappa^2A^2 \end{cases} \tag{3.8}$$

The solution to (3.7) may be written in the form

$$\frac{\partial \bar{\psi}}{\partial t}=B_1\sin(2\mu y)+B_2y\cos(2\mu y)+C_1e^{ry}+C_2e^{-ry} \tag{3.9}$$

where

$$\begin{cases} B_1=-\dfrac{2\alpha}{\mu}\cdot\dfrac{\kappa^2A^2}{4+r^2/\mu^2}+\dfrac{8\alpha}{\mu}\cdot\dfrac{\kappa^2A^2}{(4+r^2/\mu^2)^2} \\ B_2=-2\alpha\cdot\dfrac{\kappa^2A^2}{4+r^2/\mu^2}\cdot \end{cases} \tag{3.10}$$

and where C_1 and C_2 are arbitrary constants to be determined from the boundary conditions

$$\frac{d}{dy}\left(\frac{\partial \bar{\psi}}{\partial t}\right)=0,\quad y=\pm W. \tag{3.11}$$

Differentiating (3.9) with respect to y and using (3.11) we arrive at a determination of C_1 and C_2 resulting in the values:

$$C_1=-C_2=\frac{1}{r}\cdot\frac{2\mu B_1+B_2}{2\cosh(rW)}\cdot \tag{3.12}$$

Using (3.12) we can finally write the complete solution

$$\frac{\partial \bar{\psi}}{\partial t}=B_1\sin(2\mu y)+B_2y\cos(2\mu y)+\frac{2\mu B_1+B_2}{r}\cdot\frac{\sinh(ry)}{\cosh(rW)} \tag{3.13}$$

The main problem which we have in this section is to illustrate the difference between the non-divergent and divergent barotropic models. We shall therefore first consider the tendency in the mean zonal wind for the non-divergent model. This tendency can be computed from the expression

$$\frac{\partial \bar{u}}{\partial t}=-\frac{\partial \overline{u'v'}}{\partial y} \tag{3.14}$$

Corresponding to (2.6). The solid curve in figure 1 illustrates the tendency computed in m. sec.$^{-1}$ day^{-1}. The following values of the parameter were used:

1. $W=1/3\times 10^7$m., $2W\simeq 60°$ of latitude

2. $\kappa A=v_{\max}=20$ m. sec.$^{-1}$

3. $\alpha=1/(4W)$, corresponding to a slope of $\pm$ ½ of the trough and ridge lines for $y=\mp W$

It is seen that the changes predicted by the non-divergent, one-parameter model will give an increase of the wind in the middle latitudes and a decrease to the north and south. This distribution corresponds very much to the errors in the non-divergent forecasts.

We are next going to compute the changes in the mean zonal wind for the divergent, one-parameter model. Referring back to (2.8) it is seen that they may be computed from the expression:

$$\frac{\partial \bar{u}}{\partial t}=-\frac{\partial \overline{u'v'}}{\partial y}+f_0\bar{v} \tag{3.15}$$

As the first term on the right side of (3.15) is the same as the term already computed in (3.14) we may compute the term $f_0\bar{v}$ which will be a measure of the difference between the non-divergent and the divergent one-parameter models. In order to compute $\bar{v}$ we make use of the

continuity equation averaged along latitude circles. This equation is

$$\frac{\partial \bar{v}}{\partial y}+\frac{\partial \bar{\omega}}{\partial p}=0 \tag{3.16}$$

which in integrated form becomes

$$\bar{v}=-\int_{-W}^{y}\frac{\partial \bar{\omega}}{\partial p}dy \tag{3.17}$$

where we have used the boundary condition $\bar{v}=0$ for $y=-W$.

An expression for $\partial\bar{\omega}/\partial p$ may be obtained from the adiabatic equation, which for this simple model takes the form (Wiin-Nielsen [11]):

$$\frac{dF(p)}{dp}\frac{\partial \psi}{\partial t}+\frac{\sigma}{f_0}\omega=0. \tag{3.18}$$

Differentiation of (3.18) with respect to pressure, assuming dF/dp = constant, gives the following expression for the averaged divergence

$$\overline{\nabla\cdot\mathbf{V}}=-\frac{\partial \bar{\omega}}{\partial p}=-\frac{f_0}{\sigma^2}\frac{d\sigma}{dp}\frac{dF}{dp}\frac{\partial \bar{\psi}}{\partial t}. \tag{3.19}$$

Inserting (3.19) in (3.17) gives:

$$f_0\bar{v}=-r^2\int_{-W}^{y}\frac{\partial \bar{\psi}}{\partial t}dy;\ r^2=\frac{f_0^2}{\sigma^2}\frac{d\sigma}{dp}\frac{dF}{dp}>0. \tag{3.20}$$

We are now able to compute the influence of the mean meridional circulation on the tendency of the mean zonal wind. We have to use the expression (3.13) for the tendency of the zonally-averaged stream function, insert in (3.20), and perform the integration. The result of this procedure may be written:

$$f_0\bar{v}=-r^2\left[\frac{1}{2\mu}\left(\frac{B_2}{2\mu}-B_1\right)(1+\cos 2\mu y)+\frac{B_2}{2\mu}y\sin 2\mu y+\frac{2\mu B_1+B_2}{r^2\cosh(rW)}\cdot(\cosh(ry)-\cosh(rW))\right] \tag{3.21}$$

By a substitution of $y=+W$ it is seen that the other boundary condition $\bar{v}=0$ for $y=W$ is automatically satisfied.

The contribution of the implied mean meridional circulation to the change in the mean zonal wind is given in figure 1 as the dashed curve. The parameters used for computation of this curve are the same as before. For the parameter r^2 a value of 1.5×10^{-12} m.$^{-2}$ was used. The value is the same as estimated earlier by the author [11] or about twice the value used presently in the operational forecasts.

The curves in figure 1 show that the introduction of divergence in the one-parameter model has a tendency to counteract the effects of the meridional convergence of the transport of zonal momentum. As the transport

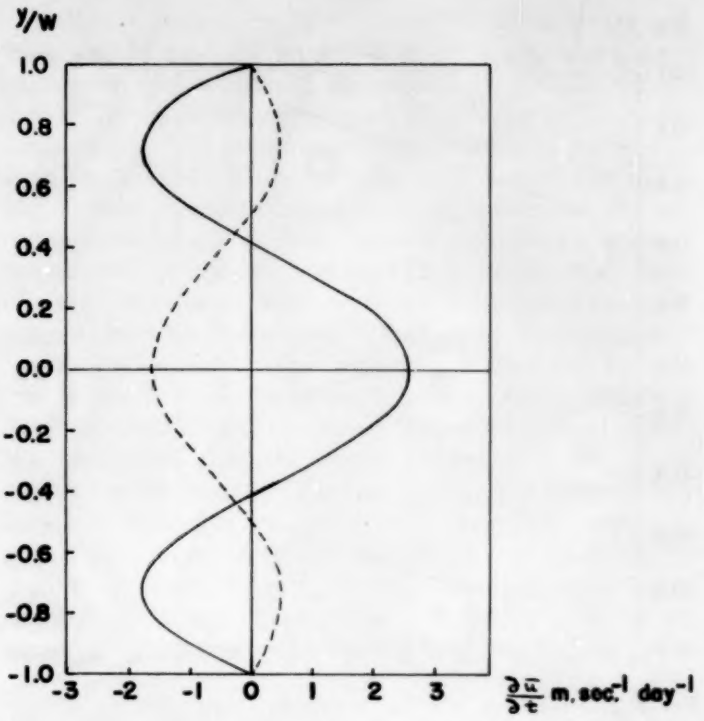

FIGURE 1.—Change in averaged zonal winds in one-parameter, divergent model in units of m. sec.$^{-1}$ day^{-1}. Solid curve is change due to convergence of meridional transport of momentum, dashed curve is change due to mean meridional circulations.

of momentum, which is the only factor in a non-divergent model, gives errors with a distribution very similar to the change caused by the momentum transport, we can expect that the errors in the mean zonal winds will be reduced in a divergent, one-parameter model.

If the idealized flow pattern treated in this section were characteristic of the atmospheric flow pattern we could expect a reduction of the error amounting to 1–2 m. sec.$^{-1}$ day^{-1}, which is roughly the order of magnitude of the present errors.

An extended series of one-parameter forecasts made with and without the contribution from the divergence does not exist. A comparison of the monthly mean errors of the averaged zonal wind for months when the divergent model has been used, with the corresponding months a year earlier when the non-divergent model was in operation, shows some reduction of the errors, but not of a magnitude comparable to that computed in our examples. The reason for this may be that the example chosen here is too extreme, especially with respect to the slope of the trough and ridge lines. It should, however, be remembered that the operational value of r^2 is about half the value chosen in the present idealized computation. Further, it is worthwhile to mention, that if an error of the present type exists in a forecast the error is likely to increase in time due to the feedback mechanism between the mean zonal current and the perturbations (see discussion in the introduction).

545014—60——3

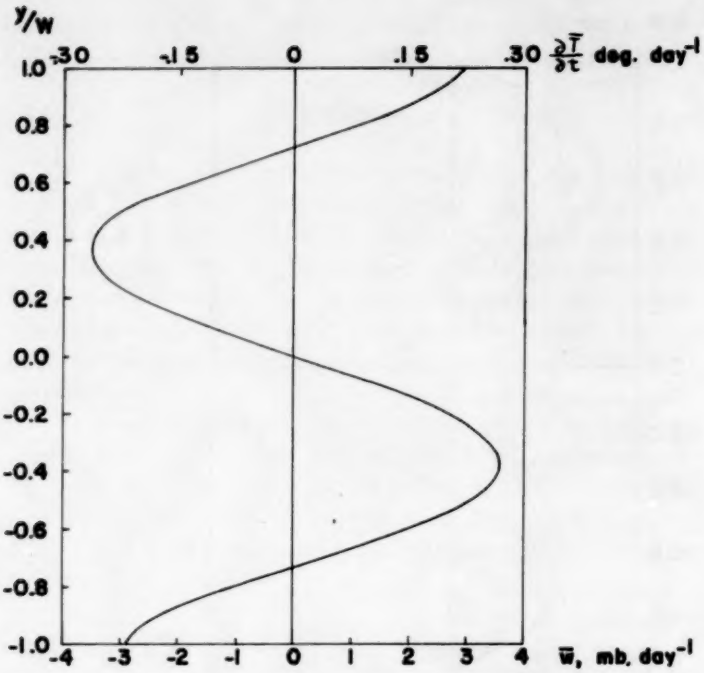

FIGURE 2.—Vertical velocity, $\omega=dp/dt$, averaged along latitude circles in one-parameter divergent model. Units: mb. day^{-1} (lower scale). Changes in zonally-averaged temperatures in the same model. Units: deg. day^{-1} (upper scale).

It is interesting to compute the implied vertical velocity averaged along the latitude circles. This can be done from equation (3.18) in an averaged form. We find

$$\bar{\omega}=-\frac{f_0}{\sigma}\frac{dF}{dp}\frac{\partial \bar{\psi}}{\partial t}. \tag{3.22}$$

$\bar{\omega}$ is given as a function of "latitude" in figure 2 using numerical values of the parameters as before. The value of the coefficient $(-f_0/\sigma)(dF/dp)$ becomes 4×10^{-7}. The units for $\bar{\omega}$ are mb. day^{-1}. It is interesting to note that the distribution of $\bar{\omega}$ gives the classical picture of three meridional cells with two direct cells to the north and south and an indirect cell in the middle latitudes. The intensity of the cells may be measured by the maximum vertical velocity, which is about 3.5 mb. day^{-1} or roughly 0.5 mm. sec.$^{-1}$.

In an investigation by Phillips [7] of a two-parameter, quasi-geostrophic model it was shown that essentially the same mean vertical velocity was implied. Phillips investigated a flow pattern with no tilt and showed that the implied mean vertical motion was due to the baroclinic unstable waves, where the isotherms are lagging behind the contours. The flow pattern considered here is such that the isotherms are always parallel to the contours at the level considered. The implied mean vertical velocity is here due to the tilt of the systems and the requirement that the temperature advection should vanish. It seems therefore that the divergent, one-parameter model contains quite realistic features in this respect.

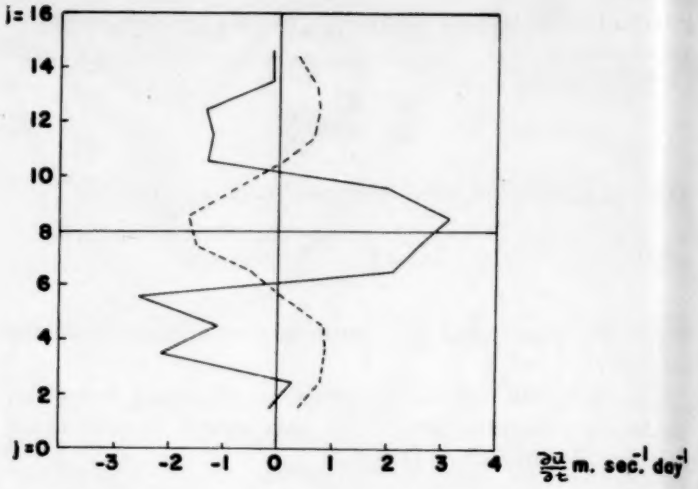

FIGURE 3.—Changes in averaged zonal winds at 500 mb. in Phillips' general circulation study. Solid curve is change due to convergence of meridional transport of momentum, dashed curve is change due to surface friction. Units: m. sec.$^{-1}$ day^{-1}.

The use which has been made of the adiabatic equation in the construction of this model implies certain temperature changes at the level where the model is used. The zonally-averaged temperature changes are due only to the mean vertical velocity, because the horizontal advection of temperature is disregarded at the level. We may easily compute these temperature changes from the equation

$$\frac{\partial}{\partial t}\left(\frac{\partial \bar{\phi}}{\partial p}\right)+\sigma\bar{\omega}=0 \tag{3.23}$$

which through use of the hydrostatic relationship reduces to

$$\frac{\partial \bar{T}}{\partial t}=\left(\frac{\sigma p}{R}\right)\bar{\omega}. \tag{3.24}$$

We find of course that the zonally averaged temperature change is proportional to the vertical velocity. The curve in figure 2 may therefore also be considered as illustrating the change in zonally averaged temperature. The value of the proportionality factor is $\sigma p/R=0.73$ at 500 mb. The maximum change in zonally-averaged temperatures is therefore about 0.26 deg. day^{-1} for the values used to characterize the flow pattern.

We shall next compare the results obtained here for the simple divergent, one-parameter model with the result obtained by a model which contains the effects of surface friction and diabatic heating. Phillips [8] has in his general circulation experiment obtained values for the important terms in the zonal momentum budget for the two levels (750 and 250 mb.) and for the terms appearing in the thermodynamic energy equation. We shall compare our figure 1, which gives the change in zonal momentum per day due to convergence of meridional transport of zonal momentum and the meridional circulation, with figure 3,

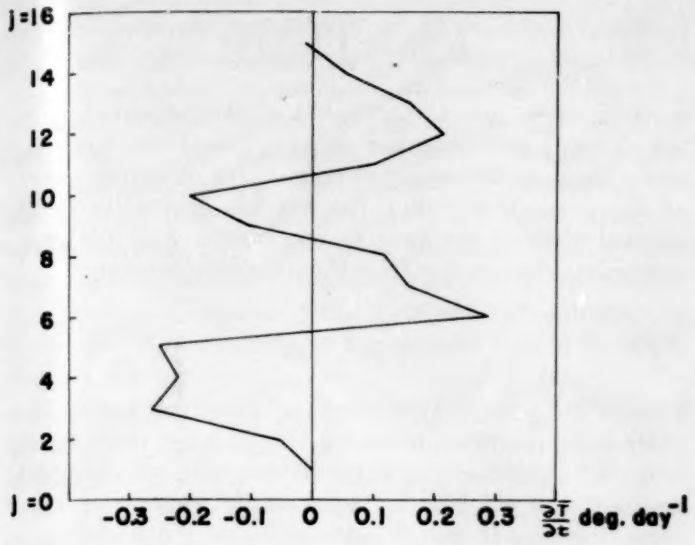

FIGURE 4.—Changes in zonally-averaged temperature at 500 mb. in Phillips' general circulation study. Units: deg. day^{-1}.

which contains the change of zonal momentum at 500 mb. in Phillips' model. The momentum budget for the 500-mb. level in his model was obtained by averaging the 250- and 750-mb. budgets, using the simple equation that

$$\frac{\partial \bar{u}_2}{\partial t}=\frac{1}{2}\left(\frac{\partial \bar{u}_1}{\partial t}+\frac{\partial \bar{u}_3}{\partial t}\right) \tag{3.25}$$

where the subscripts 1, 2, and 3 refer to 250, 500, and 750 mb. The equation becomes:

$$\frac{\partial \bar{u}_2}{\partial t}=-\frac{1}{2}\left[\frac{\partial}{\partial y}\left(\overline{u_1'v_1'}+\overline{u_3'v_3'}\right)+k\bar{u}_4\right]. \tag{3.26}$$

k is a frictional coefficient for the skin friction and u_4 the zonal wind at 1000 mb. In (3.26) we have neglected the small effect of lateral eddy viscosity used by Phillips.

The change in zonal momentum in Phillips' model at 500 mb. is due to momentum transport effects and to skin friction. The two effects are given in figure 3. Comparing figures 1 and 3 we find that the effect of meridional transport of zonal momentum acts in the same way in the two cases causing a wind increase in the middle latitudes and a decrease to the north and the south. In Phillips' model there is no effect at 500 mb. of the mean meridional circulation because of his model approximations. The effect of surface friction acts, however, opposite to the meridional transport of momentum in a way very similar to the mean meridional circulation in the model considered here. Although the divergent, one-parameter model does not have the effect of surface friction, it has an effect, which with respect to changes in mean zonal momentum acts very similar to it. Physically the two effects are very different. At every instant the frictional effect depends only on the mean zonal wind profile at the surface of the earth, while the net effect of the divergence depends upon the disturbances.

Our next problem is to compare the zonally-averaged temperature changes predicted by the divergent, one-parameter model and by the general circulation experiment. In the latter experiment the change in the mean temperature field is influenced by essentially three factors: the diabatic heating giving a cooling to the north and a warming to the south, the convergence of the meridional transport of heat, and the effect of the mean meridional circulation, disregarding again the small effect of small-scale eddy diffusion. In the model considered here we have only the effect of the mean meridional circulation. The temperature change caused by this factor is given in figure 2 (upper scale). Figure 4 gives the net effect of the three factors mentioned above. We find again that the curves in figures 2 and 4 are similar in the essential features, giving a cooling in the very low latitudes, a heating in the very high latitudes, and a strengthening of the temperature gradient in the middle latitudes. Again we are therefore tempted to conclude that the effects which are disregarded in the divergent, one-parameter model tend to balance each other with respect to changes in the zonally-averaged temperature changes.

4. TENDENCY COMPUTATIONS OF ZONAL MOMENTUM IN TWO-PARAMETER MODELS

It is generally hoped that the introduction of two or more information levels in the vertical direction will improve the short-range prediction. In this section we investigate whether we can obtain improvements in a two-parameter model in predictions of the zonal wind profile. A long record of hemispheric, two-parameter forecasts unfortunately does not exist. We therefore have to be satisfied by tendency computations.

Eliassen [5] has stressed that if the vertical structure of the atmosphere is represented by only two parameters, it becomes important to choose the two information levels with care. Eliassen represents the vertical variation of the horizontal wind by the expression

$$\mathbf{V}(x,y,p,t)=\overline{\mathbf{V}}+A(p)\mathbf{V}_T \tag{4.1}$$

where

$$\overline{\mathbf{V}}=\frac{1}{p_0}\int_0^{p_0}\mathbf{V}dp,\quad \mathbf{V}_T=\frac{1}{p_0}\int_0^{p_0}A(p)\mathbf{V}dp. \tag{4.2}$$

The two prognostic equations apply therefore to the vertically integrated flow and to the mean thermal flow in the atmosphere. If the prognostic equations are applied to specific levels in the atmosphere, Eliassen recommends choosing the two levels where $A(p)=\pm 1$ as information levels. The level where $A(p)=0$ becomes the non-divergent level. A computation leading to a determination of the function $A(p)$, based on the wind data published by Buch [2] gives the result that $A(p)=+1$ for $p=333$ mb., $A(p)=-1$ for $p=825$ mb., and $A(p)=0$ for $p=600$ mb. in winter, while the corresponding figures for his

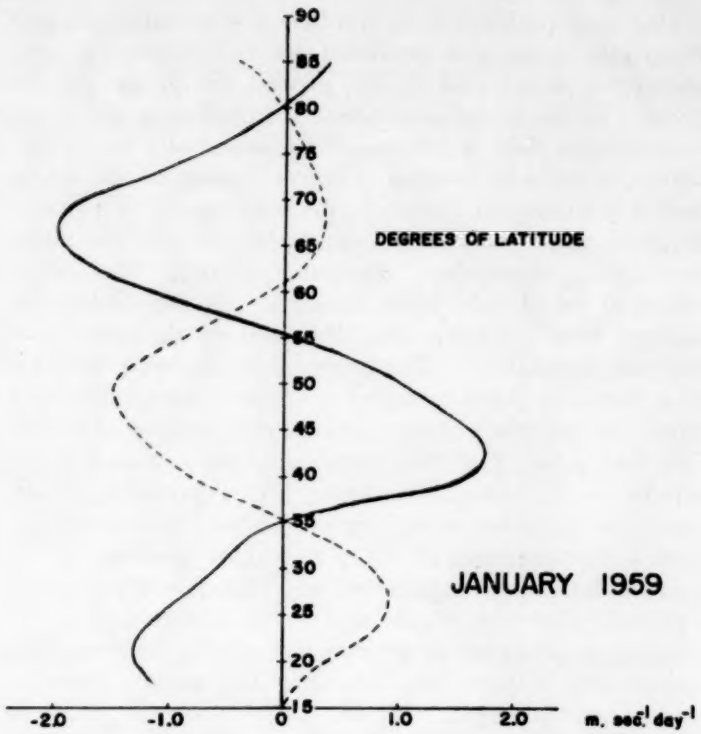

FIGURE 5.—Solid curve: 24-hour errors in mean zonal wind in operational model. Units: m. sec.$^{-1}$ day^{-1}. Dashed curve: Contributions from mean meridional circulation to changes in mean zonal winds, averaged for the month of January 1959. Units: m. sec.$^{-1}$ day^{-1}. Vertical coordinate is latitude.

summer data become: $A(p)=+1$ for $p=367$ mb., $A(p)=-1$ for $p=833$ mb., and $A(p)=0$ for $p=567$ mb. As we here intend to make a tendency computation for zonal momentum in winter, we can assume that the 600-mb. level is the non-divergent level. For our computation we will need values of the vertical motion at this level. Thompson [9] has earlier arrived at the conclusion that the non-divergent level can be approximated by the 600-mb. level. The initial vertical velocities presently computed on a daily basis apply therefore at that level.

We are next going to see how we can make a tendency computation for the zonal momentum for the 500-mb. level based upon a two-parameter model. Referring back to equation (2.3) we obtain in the frictionless case:

$$\frac{\partial \bar{u}}{\partial t}=-\frac{\partial \overline{uv}}{\partial y}+f\bar{v}-\frac{\partial \overline{u\omega}}{\partial p}. \tag{4.3}$$

We are here interested in an estimate of the contributions from the mean meridional circulation and the vertical advection of momentum to the rate of change of zonal momentum; i.e., the magnitude of the second and third terms on the right side of (4.3).

The contribution from the mean meridional circulation may be computed by a method similar to the one applied in section 3. From the continuity equation averaged along latitude circles we obtain by integration:

$$\bar{v}_5=\bar{v}_{5,b}-\int_0^y\left(\frac{\overline{\partial\omega}}{\partial p}\right)_5 dy \tag{4.4}$$

where $\bar{v}_5$ is the mean meridional wind component at 500 mb., $\bar{v}_{5,b}$ the same component at the southern boundary, and $-(\overline{\partial\omega/\partial p})_5$ the averaged component of the divergence at the same level. For the vertical derivative of the vertical velocity we have in accordance with the model approximations in the JNWP operational model:

$$\left(\frac{\partial\omega}{\partial p}\right)_5=\frac{\omega_6}{2P} \tag{4.5}$$

where $P=40$ cb. (4.5) is exact if the vertical velocity has a parabolic distribution with zero-points at 1000 and 200 mb. and an extremum value at 600 mb. It should be stressed that we get the same result with a very good approximation if we derive the vertical distribution of horizontal divergence with Eliassen's method [5]. He assumes that this distribution can be obtained from equation (4.1) simply by applying the operator $\nabla\cdot$ to both sides; i.e.

$$\nabla\cdot\mathbf{V}=A(p)\nabla\cdot\mathbf{V}_T. \tag{4.6}$$

Using the function $A(p)$ derived from Buch's [2] winter data we get $A(p_5)=0.4$.

The component $\bar{v}_{5,b}$ at the southern boundary is very difficult if not impossible to determine from the available data. In the computations to be described below it has been assumed that $\bar{v}_{5,b}=0$, which corresponds to a rigid wall at the boundary. This boundary condition does not correspond to the one in the real atmosphere nor to the one applied in the computations of the vertical velocity. A value of $\bar{v}_{5,b}$ different from zero would, however, only shift the reference point of the curves to be described later. The mean meridional velocity was therefore computed from the formula

$$\bar{v}_5=-\frac{1}{2P}\int_0^y\bar{\omega}_6 dy. \tag{4.7}$$

The vertical velocity, computed operationally, was averaged in latitude rings with a width of 5° latitude for each day of the month January 1959, as described by the author [12] in an earlier paper. $\bar{v}_5$ was then computed by a numerical integration of the expression (4.7). The results are presented in figure 5, where the contribution from the mean meridional circulation to the change in the mean zonal current is plotted as the change which would occur in $\bar{u}$ in 24 hours provided the initial mean meridional circulation persisted for this time; i.e.

$$\Delta\bar{u}_5=\Delta t\cdot f_0\cdot\bar{v}_5 \tag{4.8}$$

where $\Delta t=24$ hours.

The monthly errors in the average zonal winds for the 24-hour forecasts have been entered in the diagram on figure 5. It is obvious from figure 5 that the mean meridi-

onal circulation as computed from the procedure described above would decrease the errors in the average zonal winds in most latitudes. It accounts, at least in the monthly average presented here, for the greater part of the errors in the middle and low latitudes, while the contribution from the meridional circulation to the correction of the errors in the high latitudes is much too small, although of the correct sign. It seems therefore that a two-parameter model with the proper selection of the information levels, and especially the level where the divergence is assumed to be zero, will in the average reduce the errors found in non-divergent one-parameter forecasts. The rather small correction to the errors in the averaged zonal winds that is found in the high latitudes points in the direction that the two-parameter model predicts too small mean meridional circulations in these latitudes. This may also be expressed by saying that the level of non-divergence is lower in these high latitudes than it is farther to the south. If this is the case one will need more than two parameters to correct for the total error in the zonally-averaged winds.

The result that the level of non-divergence is lower in the high latitudes is opposite to the results obtained by Landers [6], but agrees in general with the climatological variation of the tropopause with latitude. It is reasonable to expect that the first mode of the vertical velocity in the troposphere, which is the only one used here, to a large extent is determined by the tropopause. The great similarity which is found between the mean meridional circulation derived from vertical velocities computed from a two-parameter model and the mean meridional circulation implied by the divergent one-parameter model investigated in section 3 for flow patterns with opposite tilt of trough and ridge lines in the high and low latitudes must mean that the divergent one-parameter model has a pattern of vertical velocity and divergence quite similar to that derived from a two-parameter model, at least when averaged along latitude circles.

In view of this result, suggested by the above investigation of mean meridional circulation in the two models, it is interesting and instructive to compare vertical velocities in the two models. Let us for this purpose restrict ourselves to simple harmonic waves. The vertical velocity in the divergent one-parameter model may be found from two equations:

$$\frac{\partial \nabla^2\psi_1}{\partial t}+\mathbf{V}_1\cdot\nabla(\nabla^2\psi_1+f)=q_1\frac{\partial\psi_1}{\partial t} \tag{4.9}$$

$$\omega_1=r_1\frac{\partial\psi_1}{\partial t}. \tag{4.10}$$

where $q_1=\frac{f_0^2}{\sigma^2}\frac{d\sigma}{dp}\frac{dF}{dp}$, $r_1=\frac{f_0}{\sigma}\left(-\frac{dF}{dp}\right)$. In these formulae ψ_1 is the stream function, $\mathbf{V}_1=\mathbf{k}\times\nabla\psi_1$ the horizontal wind, f_0 is a standard value of the Coriolis parameter, $\sigma=-\alpha\partial\ln\theta/\partial p$, and $F(p)$ is a function describing the variation of the horizontal wind with pressure. For the details in the derivation of equations (4.9) and (4.10) the reader is referred to an earlier paper by the author [11]. The numerical values to be used in the following are:

$$q_1=1.5\times10^{-12}\text{m.}^{-2}$$

$$r_1=\frac{3}{8}\times10^{-6}\text{ tm.}^{-3}\text{ sec.}^{-1}$$

Assume now the simple sinusoidal flow pattern to be defined by:

$$\psi_1(x,y,t)=-U_1y+A\sin\kappa(x-ct). \tag{4.11}$$

We find from (4.9) the wave-speed formula:

$$c_1=\frac{U_1-\beta/\kappa^2}{1+q_1/\kappa^2}. \tag{4.12}$$

From (4.10) we find

$$\omega_1=-r_1\cdot c_1\cdot v_1,\quad v_1=\frac{\partial\psi_1}{\partial x} \tag{4.13}$$

which combined with (4.12) leads to:

$$\omega_1=-r_1\cdot\frac{U_1-\beta/\kappa^2}{1+q_1/\kappa^2}v_1. \tag{4.14}$$

Equation (4.14) shows that we have an implied vertical motion which is upward ($\omega<0$) between trough and ridge and downward ($\omega>0$) between ridge and trough for waves with a wavelength so short that $U_1-\beta/\kappa^2$ is positive, while the opposite is true for waves with a wavelength larger than the stationary wavelength. Inserting typical values of U and v it is seen, that the implied vertical motion can obtain values of a few cm. sec.$^{-1}$. The absolute values decrease from the very short waves to the stationary wave and increase then again as the wavelength becomes larger. For comparison with a later result we shall write (4.14) in the form:

$$\omega_1=-\frac{r_1U_1}{1+q_1/\kappa^2}v_1+\frac{r_1}{1+q_1/\kappa^2}\cdot\frac{\beta}{\kappa^2}v_1. \tag{4.15}$$

This vertical velocity can be compared with the implied vertical velocity in the two-parameter model. It has been shown earlier by the author [10] that this vertical velocity is given by the expression:

$$\omega_2=-\frac{r_2(2U')}{1+q_2/\kappa^2}v_2+\frac{r_2}{1+q_2/\kappa^2}\cdot\frac{\beta}{\kappa^2}\cdot v' \tag{4.16}$$

for simple sinusoidal waves. The symbols in (4.16) have the following meaning: v_2 and v' are the meridional wind components for the mean flow and the thermal flow in the two-parameter model, while $r_2=2f_0/\sigma P$, $q_2=2f_0^2/\sigma P^2$. Comparing (4.15) with (4.16) it is seen that the first terms in the two expressions are very similar. They both give a contribution to the vertical velocity which is in phase

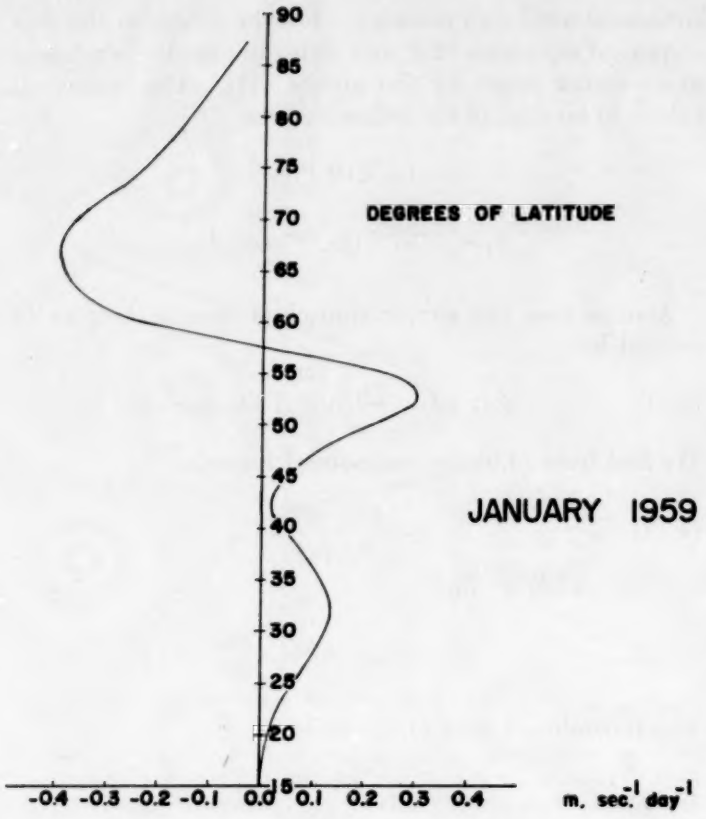

FIGURE 6.—Contribution from vertical advection of momentum to changes in the mean zonal wind as a function of latitude. Units: m. sec.$^{-1}$ day^{-1}. Averaged contribution for January 1959.

with the meridional component of the flow (v_1 and v_2). The contribution from the second term in the expression is in the one-parameter model in phase with the v_1-wave, while it is in phase with the thermal wave (v') in the two-parameter model. In the majority of cases, where the v_1-wave and v'-wave have only small phase differences, it is seen the divergent one-parameter model will imply vertical velocities that are distributed in nearly the same manner as those obtained from a two-parameter model. The magnitude of the vertical velocities will be somewhat, but not very much, different in the two models, because $r_1<r_2$, $q_1<q_2$ using values from the standard atmosphere.

We have thus in this section shown that the contribution from the mean meridional circulation (in a two-parameter model with the non-divergent level at 600 mb.) to changes in zonal momentum at 500 mb. will reduce the errors in the prediction of the averaged zonal winds in the non-divergent one-parameter model. The same conclusion was made plausible in section 3, where the divergent one-parameter model was investigated. It is *not* claimed that the contribution from the meridional circulation can explain the total error found in the prediction of the averaged zonal flow, but it has been the purpose to show that the two models which have been investigated give similar reductions of the errors. The contribution from the surface friction is naturally of importance, and it is evident that this contribution can be incorporated with greater accuracy in a two- or multi-parameter model.

5. ESTIMATES OF CONTRIBUTIONS FROM VERTICAL ADVECTION

The effects of the vertical advection term in the equations of motion, which corresponds to the vertical advection of vorticity and the twisting term in the vorticity equation, have in general not been included in the forecasts. We may get an estimate of the importance of these terms in a two-parameter model for the prediction of averaged zonal winds by a computation of the last term in equation (4.3), which can be estimated using the vertical velocities computed operationally. It may be argued that the vertical velocities are computed from a model not containing these terms. It should be pointed out that although this argument is true with regard to predictions, it does not apply initially, because the contribution from the vertical advection of vorticity and the twisting cancel out in the thermal vorticity equation in a two-parameter model. Initially, we will therefore have the same vertical velocities. The term in question may be approximated in a way similar to the one applied in section 4. We get:

$$\left(\frac{\partial\overline{\omega u}}{\partial p}\right)_5=-\left(\overline{u_5\frac{\omega_6}{2P}}-\overline{\omega_5\frac{u_T}{\Delta p}}\right) \tag{5.1}$$

where $P=40$ cb., u_T is the zonal component of the thermal wind between 850 and 500 mb., $\Delta p=35$ cb., and the subscripts denote the level where the quantities are measured. The contribution from both of these terms to the change in the zonal wind can easily be computed from the available data. At each grid point we have to form the product of the vertical velocity and the zonal component of the 500-mb. wind and the thermal wind, respectively. These products are then averaged in the latitude rings and the results expressed as changes in the averaged zonal winds in a 24-hour period. The result of these computations is shown in figure 6 for the month of January 1959. The magnitude of the contribution from the vertical advection terms is first of all smaller than that from the convergence of the meridional transport of momentum and the mean meridional circulation. Secondly, we find that the vertical advection of momentum is not distributed in such a way as to reduce the errors in the non-divergent, one-parameter model. The obvious conclusion from this computation is that the contribution from the vertical advection of momentum will not improve the forecast of zonally averaged winds on the average in a two-parameter model. The effect is definitely of smaller magnitude than the other effects in equation (4.3), and it is likely that a better resolution in the vertical is needed to incorporate this effect with greater accuracy.

The term containing the vertical transport of momentum can therefore possibly be neglected in the mid-

troposphere as indicated above. However, approaching the ground the effect must become of greater importance simply because the vertical transport of momentum next to the ground is the surface stress. Considerable information regarding the importance of the surface stress for the momentum budget in the lower layers has been computed by Phillips [8].

6. GENERAL CONCLUSIONS

The ability of one- and two-parameter models to predict changes in averaged zonal winds has been investigated. It has been found that the divergent, one-parameter model will reduce the errors found in non-divergent, one-parameter predictions in the average due to the implied mean meridional circulations found in flow patterns where the trough and ridge lines have opposite tilts in the low and high latitudes.

Tendency computations of changes in zonally averaged winds have been performed using initial values of vertical velocities computed from a frictionless, two-parameter model with no divergence at 600 mb. It is found that the mean meridional circulation in this model also would reduce the errors found in the non-divergent, one-parameter predictions in the average. One result of this part of the study is that it is very important to choose the information levels properly, if a two-parameter model is used. As the contribution from the surface friction also seems to be important for the budget of zonal momentum even in short-range prediction, and because the surface flow is difficult to represent with good accuracy in a two-parameter model, it is likely that more than two parameters will be necessary to predict changes in zonal momentum correctly.

ACKNOWLEDGMENTS

The author would like to thank Mrs. Margaret McLaughlin for the coding of the computations in sections 4 and 5.

REFERENCES

1. C. L. Bristor, "Zonal Wind Errors in the Barotropic Model," *Monthly Weather Review*, vol. 87, No. 2, Feb. 1959, pp. 57–63.
2. H. S. Buch, "Hemispheric Wind Conditions During the Year 1950," Final Report, Part 2, Contract AF19(122)–153, Dept. of Meteorology, Massachusetts Institute of Technology, 1954, 126 pp.
3. G. P. Cressman, "Barotropic Divergence and Very Long Atmospheric Waves," *Monthly Weather Review*, vol. 86, No. 8, Aug. 1958, pp. 293–297.
4. G. P. Cressman, "An Operational Objective Analysis System," *Monthly Weather Review*, vol. 87, No. 10, Oct. 1959, pp. 367–374.
5. A. Eliassen, "A Procedure for Numerical Integration of the Primitive Equations of the Two-Parameter Model of the Atmosphere," Final Report, Contract AF19(604)–1286, Dept. of Meteorology, University of California at Los Angeles, 1956, 53 pp.
6. H. Landers, "A Three-Dimensional Study of the Horizontal Velocity Divergence," *Journal of Meteorology*, vol. 12, No. 5, Oct. 1955, pp. 415–427.
7. N. A. Phillips, "Energy Transformations and Meridional Circulations Associated with Simple Baroclinic Waves in a Two-Level, Quasi-Geostrophic Model," *Tellus*, vol. 6, No. 3, Aug. 1954, pp. 273–286.
8. N. A. Phillips, "General Circulation of the Atmosphere: A Numerical Experiment," *Quarterly Journal of the Royal Meteorological Society*, vol. 82, No. 352, April 1956, pp. 123–164.
9. P. D. Thompson, "Statistical Aspects of the Dynamics of Quasi-Nondivergent and Divergent Baroclinic Models," *C.-G. Rossby Memorial Volume*, Stockholm, 1959, pp. 350–358.
10. A. Wiin-Nielsen, "On Certain Integral Constraints for the Time-Integration of Baroclinic Models," *Tellus*, vol. 11, No. 1, Feb. 1959, pp. 45–59.
11. A. Wiin-Nielsen, "On Baratropic and Baroclinic Models, with Special Emphasis on Ultra-Long Waves," *Monthly Weather Review*, vol. 87, No. 5, May 1959, pp. 171–183.
12. A. Wiin-Nielsen, "A Study of Energy Conversion and Meridional Circulation for the Large-Scale Motion in the Atmosphere," *Monthly Weather Review*, vol. 87, No. 9, Sept. 1959, pp. 319–332.
13. P. M. Wolff, "The Error in Numerical Forecasts Due to Retrogression of Ultra-Long Waves," *Monthly Weather Review*, vol. 86, No. 7, July 1958, pp. 245–250.

ON A SPECIAL DISTRIBUTION OF MAXIMUM VALUES[1]

RAYMOND SNEYERS

Institut Royal Météorologique de Belgique, Uccle, Belgium

[Manuscript received December 8, 1959]

ABSTRACT

The classical extreme-value theory does not give a good account of the distribution of maximum rainfall intensities in Belgium. Reasons are given for the use, in this case, of a probability function defined by a double exponential whose argument is a function represented by a curve with two asymptotes. The application of such a probability function, when the curve is a branch of a hyperbola, to the maximum rainfall, in 1 min., at Uccle, leads to a good fit.

1. INTRODUCTION

All problems concerned with water streaming during rainfall have generally to be solved with the knowledge of probabilities of rainfall intensities. Consequently, it is of some importance to be able to make statistical prediction of such variates with the best possible accuracy.

This paper will be more especially concerned with the monthly maximum rainfall intensities in 1 min. provided at Uccle, Belgium (Institut Royal Météorologique) by a Hellmann rain recorder.

2. EXTREME-VALUE DISTRIBUTION FUNCTIONS

The estimation of the proabilities of maximum rainfall intensities belongs obviously to extreme-value theory and therefore it should be remembered what kind of distribution functions are ordinarily best fitted to such data, functions which were introduced by Fisher and Tippett [1].

If t is the variate and if $\phi(t_o)$ gives the probability that t is less than the fixed value t_o, these distribution functions are defined by the equation:

$$\phi(t)=\exp\,[-e^{-y}]$$

where $y=ax+b$, with a and b constant and $a>0$, and with:

type I: $x=t$ when $-\infty\leq t\leq\infty$

type II: $x=\log t$ when $0\leq t\leq\infty$

type III: $x=\log(-t)$ when $-\infty\leq t\leq 0$

There are still other forms, but they are all derived from the above types by linear transformation. Different methods of adjustment exist and all actually known have been recently reported by Gumbel [2]. The easiest one consists in adjusting by least squares $y=-\log\,(-\log F)$, where F is the observed cumulative frequency distribution, to a linear function of x.

3. MONTHLY MAXIMUM INTENSITIES IN 1 MIN., AT UCCLE

Our investigation was made on the maximum intensities observed during the period 1938–57. More precisely, the maximum rainfall intensity was determined for every month of each year of this period and the means of those monthly maximums were calculated for each month. Frequency distributions were then established with the use of class intervals having a width of one-fifth of the mean monthly maximum.

The 12 samples obtained in this way looked very similar and suggested the assumption of an identical theoretical

TABLE 1.—*Monthly maximum rainfall intensities in 1 min., at Uccle, Belgium. t is given in fifths of the mean of the monthly maximum intensity*

t	Observed and adjusted frequency distributions						
	$F(t)$	$x=\log_{10}t$ 10^{-2}	y 10^{-2}	y' 10^{-2}	$\phi(t)=\exp[-e^{-y'}]$	$z=y-y'$ 10^{-2}	z' 10^{-2}
1.5	0.0672	18	−99	−182	0.002	83	83
2.5	.2227	40	−41	−062	.156	21	20
3.5	.4076	54	11	014	.419	−3	−4
4.5	.5373	65	48	074	.621	−26	−24
5.5	.6597	74	88	122	.744	−34	−33
6.5	.7437	81	122	160	.817	−38	−37
7.5	.8403	88	175	198	.871	−23	−28
8.5	.8613	93	190	226	.901	−36	−38
9.5	.8866	98	212	253	.923	−41	−35
10.5	.9202	102	249	274	.937	−25	−31
11.5	.9412	106	280	296	.950	−16	−26
12.5	.9580	110	315	318	.959	−3	−20
13.5	.9622	113	326	334	.965	−8	−14
14.5	.9706	116	351	351	.970	0	−8
15.5	.9790	119	385	367	.975	18	−1
18.3	.9832	126	408	405	.983	3	20
19.6	.9874	129	437	421	.9853	16	31
21.4	.9916	133	478	443	.9882	35	45
24.0	.9958	138	547	470	.9909	77	67

[1] This paper was presented and discussed at a Special Climatological Seminar, U.S. Weather Bureau, on April 16, 1959.

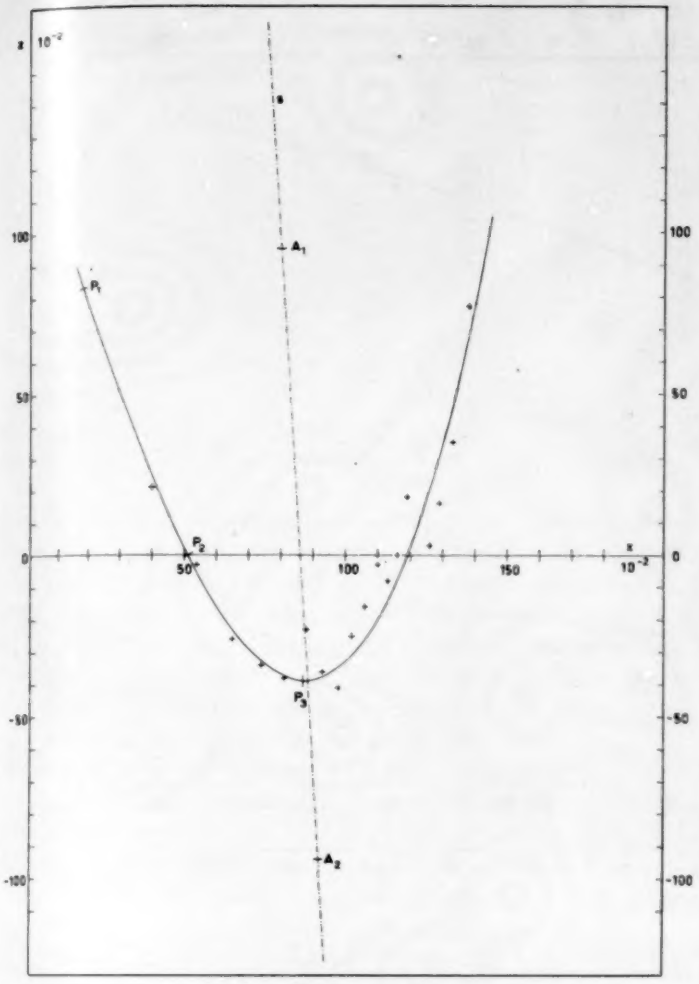

FIGURE 1.—Variation of z as a function of x. Adjusted curve and observed values.

distribution. This assumption was tested and found acceptable and therefore all data were grouped in one sample.

The cumulated frequency distribution $F(t)$ derived in that manner, t being given in fifths of the mean monthly maximum, appears in table 1. It was obtained by dividing the cumulated number of occurrences by $(n+1)$, n being the size of the total sample (here $n=237$, because no maximum rainfall intensity was measured during three of the 240 months of the considered period).

The intensities being essentially non-negative, it is clear that the adjusted function which has to be tried is a Fisher-Tippett type II distribution. Therefore we have to take $x=\log t$, or more conveniently: $x=\log_{10} t$, and to adjust $y=-\log(-\log F)$ to x.

The values of y were obtained from the Probability Tables [3] and the equation:

$$y'=5.43\,x-279.36 \tag{1}$$

was found with adjusting y to x by the ordinary method of least squares. The values of x, y, y', and $\phi(t)=\exp[-e^{-y'}]$ are also given in table 1.

The goodness of fit was tested with the Kolmogorov-Smirnov test [4] and the χ^2 test. For the first one, the differences $|F(t)-\phi(t)|$ were calculated and the largest difference compared with its critical value d. In this case the largest difference is 0.084 and, at the 0.05 level, $d=1.36/\sqrt{237}\simeq 0.088$. Since we are concerned with grouped data and an adjusted theoretical distribution, the largest difference seems to be too near its critical value to be considered as non-significant. Moreover, the χ^2 test leads to a value of χ^2 which is significant at a level smaller than 5×10^{-4}. The adjustment has thus to be rejected.

4. ADJUSTMENT OF y TO x WITH THE USE OF A QUADRATIC RELATIONSHIP

The reasons for this rejection are apparently related to a systematic variation of y with respect to y', a variation which is made evident by plotting the differences $z=y-y'$ against x (see fig. 1). In addition, this graphical representation suggests an asymptotic linear variation for small and for large values of x, variations which, in the simplest case, might be represented by a branch of a hyperbola. Such an asymptotic behavior of y had however to be expected here. It has, in fact, to be remembered that in Belgium, maximum intensities are provided by two kinds of rains, the first kind being the continuous rains falling during the passage of cyclones, and the second one being the showers accompanying certain polar air invasions as well as thunderstorms. In terms of probabilities, this means that the observed maximum is the largest between two extreme values, each of them being issued from a different population. Therefore, if $F_1(t)$ and $F_2(t)$ are the cumulative distribution functions of each population of maximums, it is clear that $\phi(t)=F_1(t)\times F_2(t)$ will be the cumulative distribution function of the largest of the two maximums. If, moreover, large values of the first population are small values of the second one, it may be expected that for the largest values of t, $\phi(t)$ will vary like $F_2(t)$, since for such values of t, $F_1(t)$ is very near to 1, and that for the smallest values of t, $\phi(t)$ will vary like $F_1(t)$, since $F_2(t)$ remains then very near to zero.

Now if we choose a branch of a hyperbola to represent such a variation of y, the adjustment has to be made with an equation of the following type:

$$y=ax+b+\epsilon\sqrt{c^2(x-d)^2+e^2},\ \text{with}\ \epsilon=\pm1, \tag{2}$$

where $a>|c|$, since the derivative dy/dx has to remain positive for any x, and where ϵ equals $+1$ or -1, according as the curvature of the curve is set toward the positive or the negative values of y.

In our case, the adjustment was performed on the differences z, and graphical estimation was preferred to a least squares procedure because the last method does not take in account the fact that all the values of z do not have the same precision. Therefore a first sketch of the

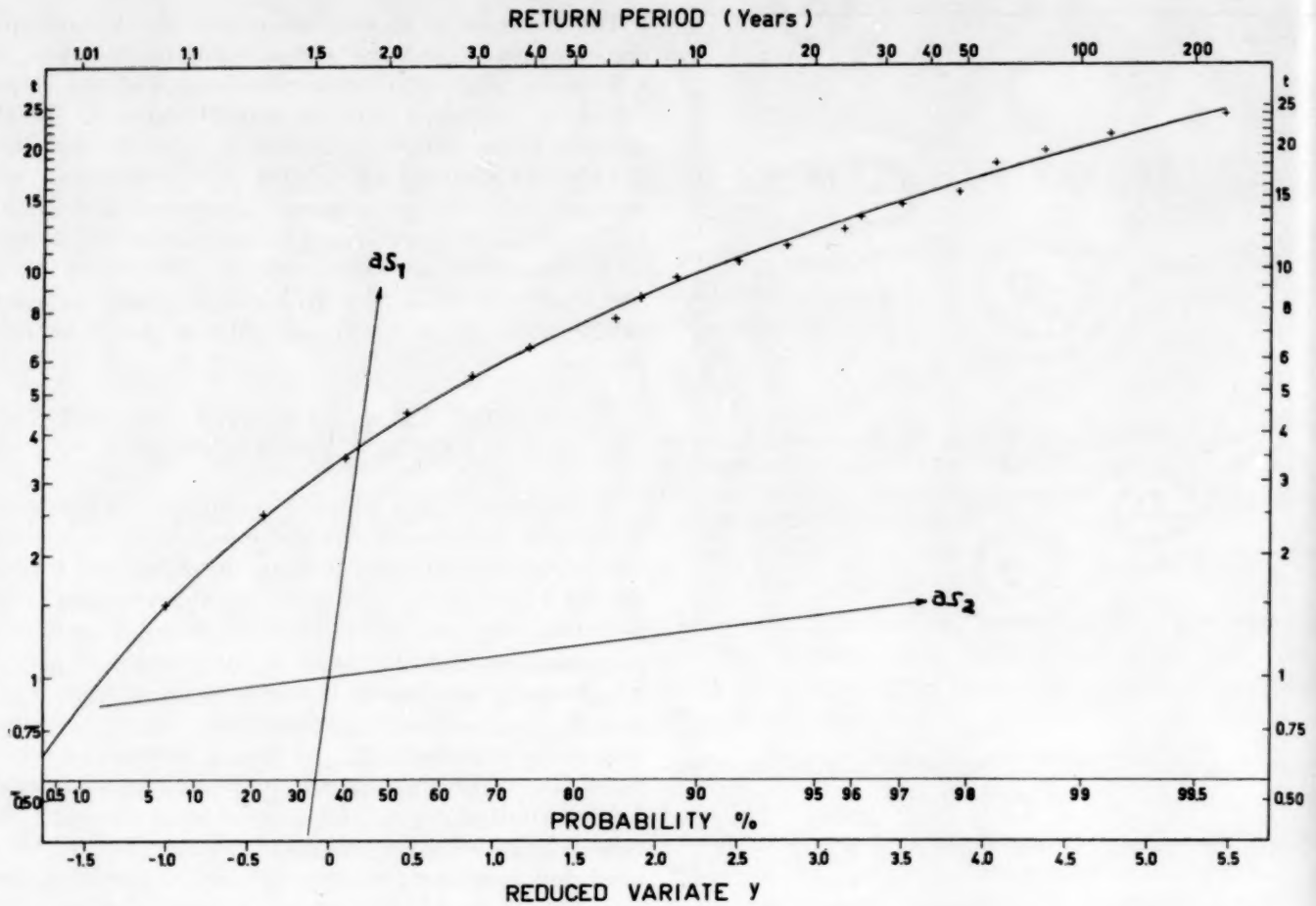

FIGURE 2.—Distribution of the monthly maximum rainfall intensities in 1 min., at Uccle. Adjusted curve and observed values. t is given in fifths of the mean monthly maximum.

curve was drawn and a graphical estimation of its axis of symmetry s was made. Using then the points $A_1(x=80, z=95)$ and $A_2(x=92, z=-94)$, the equation of this axis was found to be:

$$z+15.75\,x-1355=0. \tag{3}$$

With this result the equation of the hyperbola may be written in the form:

$$(z+15.75x-1355)^2-\alpha^2(z-0.0635x+\beta)^2=\gamma \tag{4}$$

where α, β, and γ are constants; note that $(15.75)^{-1}=0.0635$.

Finally, taking in account that the points $P_1(x=18, z=83)$, $P_2(x=51, z=0)$, and $P_3(x=87, z=-39)$ are on the curve, it is found that $\alpha^2=4.3031$, hence:

$$\alpha=2.074;\ \beta=879.20;\ \text{and}\ \gamma=-2{,}997{,}366. \tag{5}$$

Whence:

$$z=4.85x-1{,}555.8+\sqrt{98.6(x-141.3)^2+908{,}017} \tag{6}$$

or, with (1):

$$y=10.28x-1835.2+\sqrt{98.6(x-141.3)^2+908{,}017} \tag{7}$$

Since 10.28 is larger than $\sqrt{98.6}$, the branch of hyperbola defined by (7) may be accepted.

The values of z' calculated with (6) are given in table 1 too, while both the distribution $\phi_1(t)$ defined by (7) and the observed distribution have been drawn in figure 2; this time, the comparison indicates a very good fit, which is confirmed by a value of χ^2 for which $P>0.20$.

In figure 2, the asymptotic directions as_1 and as_2 have also been drawn; they were derived from the equation:

$$y-(10.28\pm\sqrt{98.6})x=0.$$

5. FINAL REMARKS AND CONCLUSION

As was mentioned above, a relatively large sample was obtained by grouping in one sample the different samples corresponding to each month. Although the assumption permitting such a grouping was found to be acceptable, it is not uninteresting to make a last comparison in order to verify if this assumption is quite

TABLE 2.—*Differences between the theoretical distribution $\phi_1(t)$ and the observed distributions by seasons F_{I-III}, F_{IV-VI}, F_{VII-IX}, and F_{X-XII}. t is given in fifths of the mean monthly maximum intensity.*

t	$\phi_1(t)$	ΔF_{I-III}	ΔF_{IV-VI}	ΔF_{VII-IX}	ΔF_{X-XII}
1.5	0.067	0.054	−.034	−.034	0.015
2.5	.232	.096	−.084	−.068	.014
3.5	.397	.120	−.020	−.085	.013
4.5	.545	.058	−.037	−.086	.013
5.5	.663	.027	.026	−.089	−.007
6.5	.747	−.006	.024	−.042	−.025
7.5	.816	.029	.004	.053	−.029
8.5	.859	.003	−.023	.027	−.039
9.5	.893		−.007	.009	−.040
10.5	.916	−.037	−.014	.019	.002
11.5	.935	−.021	−.017	.016	.000
12.5	.950		.001		.018
13.5	.960		.008		
14.5	.968	−.020			
15.5	.975	−.010		−.007	
18.3	.986				−.002
19.6	.989		−.005		
21.4	.992			−.008	
24.0	.995	−.012			

justified. This comparison was made by grouping the data in four samples corresponding respectively to the quarters January–March (I–III), April–June (IV–VI), July–September (VII–IX), and October–December (X–XII), and by calculating the differences of the observed frequency distributions for each of these periods from the theoretical distribution $\phi_1(t)$ defined by (7).

The results are given in table 2. They show that the fit is best for the quarter October–December, and less good for the other ones with, in particular, higher probabilities for small values of t during the period January–March and, on the contrary, lower probabilities for such values during the period April–September. A better fit is thus to be expected if each group is treated separately.

However, for high values of t, it should be noted that the fit is very good in the four cases. This last statement may be illustrated by the following feature:

It was formerly admitted that the intensity in 1 min. at Uccle might be considered as a maximum which would never occur. In reality, the probability of having in the year an intensity less than 5 mm. in 1 min., computed from the probabilities of such an intensity occurring during any month of the year, leads with the use of $\phi_1(t)$ to a probability of 0.9665. With other words, an intensity of at least 5 mm. in 1 min. has a return period of about 30 years.

Another estimation of this return period has been made by adjusting a Fisher-Tippett type I distribution to the sample of 20 yearly maximums observed during the period 1938–1957. More precisely, the procedure described by Gumbel [2] p. 226, leads to the relation:

$$x=10.07y+14.78 \tag{8}$$

where x is given in tenths of millimeters which, for $x=50$, gives $y=3.498$, namely a probability of 0.9702 and a return period of 33.6 years, both in very good agreement with our first estimation.

Furthermore, the secular maximum estimated in the same manner was found to be 6.17 mm. by the first method (practically in July), while $y=4.60$ in (8) leads to $x=6.11$ mm. The agreement is again excellent.

To conclude, the favorable results obtained by the very simple computations described above advocate the use of the considered double exponential each time that extreme values may come from at least two sufficiently different populations.

ACKNOWLEDGMENTS

The writer wishes to express his gratefulness to Dr. H. E. Landsberg, Director, and to Mr. H. C. S. Thom, Chief Climatologist, Office of Climatology, U.S. Weather Bureau, who kindly allowed and organized the Special Climatological Seminar at the Office of Climatology, where this paper was presented and discussed.

REFERENCES

1. R. A. Fisher and L. H. C. Tippett, "Limiting Forms of the Frequency Distribution of the Largest or Smallest Member of a Sample," *Proceedings, Cambridge Philosophical Society*, vol. 24, 1928, pp. 180–190.
2. E. J. Gumbel, *Statistics of Extremes*, Columbia University Press, New York, 1958.
3. U.S. National Bureau of Standards, "Probability Tables for the Analysis of Extreme-Value Data," *Applied Mathematics Series* No. 22, 1953.
4. F. J. Massey, "The Kolmogorov—Smirnov Test for Goodness of Fit," *Journal, American Statistical Association*, vol. 46, 1951, pp. 68–78.

WEATHER NOTE

NIGHTTIME TEMPERATURE RISES IN MOUNTAIN CANYONS

G. F. VON ESCHEN

U. S. Weather Bureau, Albuquerque, N. Mex.

[Manuscript received February 8, 1960]

"Is it true that in Cochiti Canyon (northern New Mexico) the temperature frequently rises as much as 20° around midnight?" This question was asked some time ago and in my reply I pointed out that we had no actual records that would substantiate such a temperature rise and that such rises would probably occur only under certain rather rare meteorological conditions.

In late 1958 a thermograph was installed at the climatological substation at Tijeras Ranger Station and we now have a year's thermograph record for that station. The Tijeras Ranger Station is located in Cedro Canyon in the Manzano mountains, some 15 miles east of Albuquerque. The maximum and minimum thermometers and the thermograph are exposed in a standard instrument

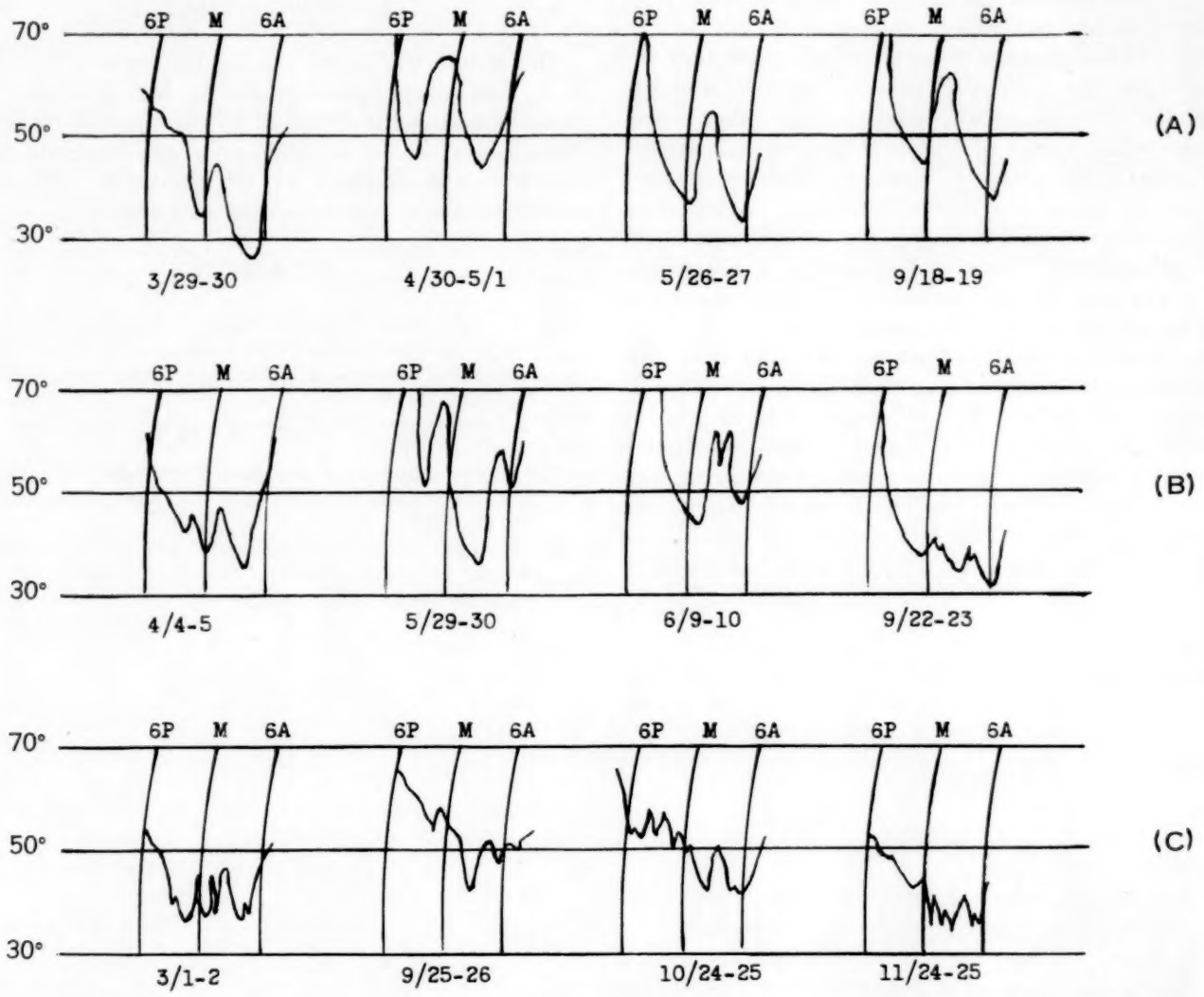

FIGURE 1.—Tracings of thermograph records made at Tijeras Ranger Station, N. Mex., during 1959, showing nighttime temperature rises.

shelter in an open site on the floor of the canyon at an elevation of 6,300 feet above sea level. Cedro Canyon, running in a general south to north direction, is a narrow, winding canyon with mountain ridges some 1,000 to 2,000 feet higher, paralleling either side. There is a fall of about 800 feet from the head of the canyon to the site of the station, a distance of some 4 miles in a straight line. The station is about one-half mile from the mouth of the canyon where it joins Tijeras Canyon. This latter canyon runs from northeast to southwest and opens onto the wide Rio Grande Valley just east of Albuquerque and about 10 miles below the confluence of the two canyons.

A review of the thermograph traces for the Tijeras Ranger Station shows a nighttime temperature rise and subsequent fall on approximately 42 percent of the days in 1959. This rise and fall in temperature during the night may vary from a few degrees to an abrupt change of as much as 20°. In figure 1 are reproduced nighttime thermograph traces for some of the more typical cases. Group (a) illustrates a single rise in temperature of considerable magnitude occurring near midnight. The period of higher temperature may last from 1 to several hours and then the temperature falls rapidly to a point that might be expected if the nighttime temperature had followed a normal diurnal curve. In group (b) two separate rises in temperature followed by falls are indicated during the night, representing two distinct and separate periods when local conditions resulted in a temperature change. In group (c) frequent temperature fluctuations are indicated illustrating the effect of numerous variations in the local conditions which produce these changes.

Wind and sky cover records are not available for the Tijeras Ranger Station but it is believed that the temperature rises are associated with air drainage and mountain-valley breezes which spring up during the night and for varying periods of time wipe out the usual nighttime valley inversions. It would also seem from groups (b) and (c) on the chart that at times these breezes are quite erratic, occasionally increasing and dying out several times during the night. A review of the weather records at Albuquerque did not show any definite type of weather associated with the temperature variations illustrated. Generally the nights at Albuquerque were clear, although on one occasion high broken to overcast sky conditions prevailed throughout the night. Winds at Albuquerque on the nights examined were generally light and variable, although on 2 nights south to southeast winds up to 20 knots were recorded.

The thermograph records at least prove that at Tijeras Ranger Station near midnight temperature rises do occur. It would seem entirely within reason that similar nighttime temperature changes also occur in Cochiti Canyon and probably in many other mountain canyons throughout the West.

THE WEATHER AND CIRCULATION OF FEBRUARY 1960

A Cold Stormy Month Over the United States Associated With Widespread Blocking

L. P. STARK

Extended Forecast Section, U.S. Weather Bureau, Washington, D.C.

1. THE WINTER SEASON

Intense blocking over North America in February was the climax of the winter season of 1959–60. In the three months of December, January, and February the patterns of circulation (fig. 1A), precipitation (fig. 1B), and temperature (fig. 1C) had large departures from normal.

The 700-mb. mean pattern for winter 1959–60 consisted of a ridge in western North America and a trough in eastern United States. Most impressive was the positive height departure from normal (hereafter referred to as DN) which reached from 40° N. to beyond the North Pole, with a center of +480 feet near Baffin Island. To the south heights were lower than normal from 40° N. to southern Mexico, a pattern typical of blocking [1].

Precipitation in the winter of 1959–60 (fig. 1B) was more than 1½ times the normal in a band from the Southwest to the Great Lakes. Relative dryness was confined to parts of the Ohio Valley and the Pacific Northwest in an otherwise rather wet map.

The departures from normal of average surface temperature (fig. 1C) were well correlated with the 700-mb. height DN (fig. 1A) and resulted from successively colder months through the season. The onset of the calendar winter was a marked contrast to the cold fall season which had preceded. December was very mild (see fig. 4 of [2]); January was considerably colder (see fig. 7A of [3]); and in February (fig. 2) there was a further increase in the intensity and extent of the cold air.

In summary the winter of 1959–60 was cold in the South and warm in the North. The season began predominantly warm and ended with a very cold February. The circulation over North America featured high latitude blocking, which in the month of February played a most interesting role.

2. THE MONTHLY MEAN CIRCULATION

The predominant feature of the circulation in February, as shown in figure 3, was the large center of positive height DN over northern North America. The maximum height departure was 660 feet near Davis Strait, and heights averaged above normal from the Great Lakes to the North Pole and from the Gulf of Alaska to the Norwegian Sea. The impact of these anomalies was of primary significance to much of the western portion of the Northern Hemisphere and especially to the weather in the United States.

The area of positive height DN was surrounded by a band of negative departures which was almost uninterrupted around the hemisphere. That particular configuration was accompanied by an expanded circumpolar vortex of the classic type [4].

A further manifestation of the southward displacement of westerlies can be derived from the profile of zonal wind speed at 700 mb. (fig. 4). The belt of westerly winds reached a maximum of almost 15 m.p.s. at latitude 30–35° N. and remained stronger than normal down to 20° N. Normally the maximum has a speed 2 m.p.s. slower than and a location 5° north of that observed this February. Note also that the westerlies were about 8 m.p.s. slower than normal in the latitude band 50–55° N., compensating for the excess westerlies in lower latitudes [1].

The time variation of the 5-day mean zonal index, giving the speed of the 700-mb. temperate westerlies (35–55° N.) from 5° W. westward to 175° E., is reproduced in figure 5 for the entire winter season. Its general trend was downward, interrupted at mid-February by a temporary recovery. Weaker than normal temperate westerlies are frequently a sign of colder than normal temperatures at mid-latitudes over continents, as was observed in February (fig. 2). In addition, below normal thicknesses from 1000 to 700 mb. (fig. 6) were almost everywhere distributed in a manner similar to height departures from normal (fig. 3).

By the end of February the 5-day mean index fell to 5.1 m.p.s., the lowest value of the month and of the season. Five-day mean temperatures were also the lowest of the season at the end of the month when they averaged from 25 to 32° F. below normal from eastern Kansas to Idaho. In general, the long-term trend of the index was downward and very much like that of the surface temperatures in the United States for the winter season.

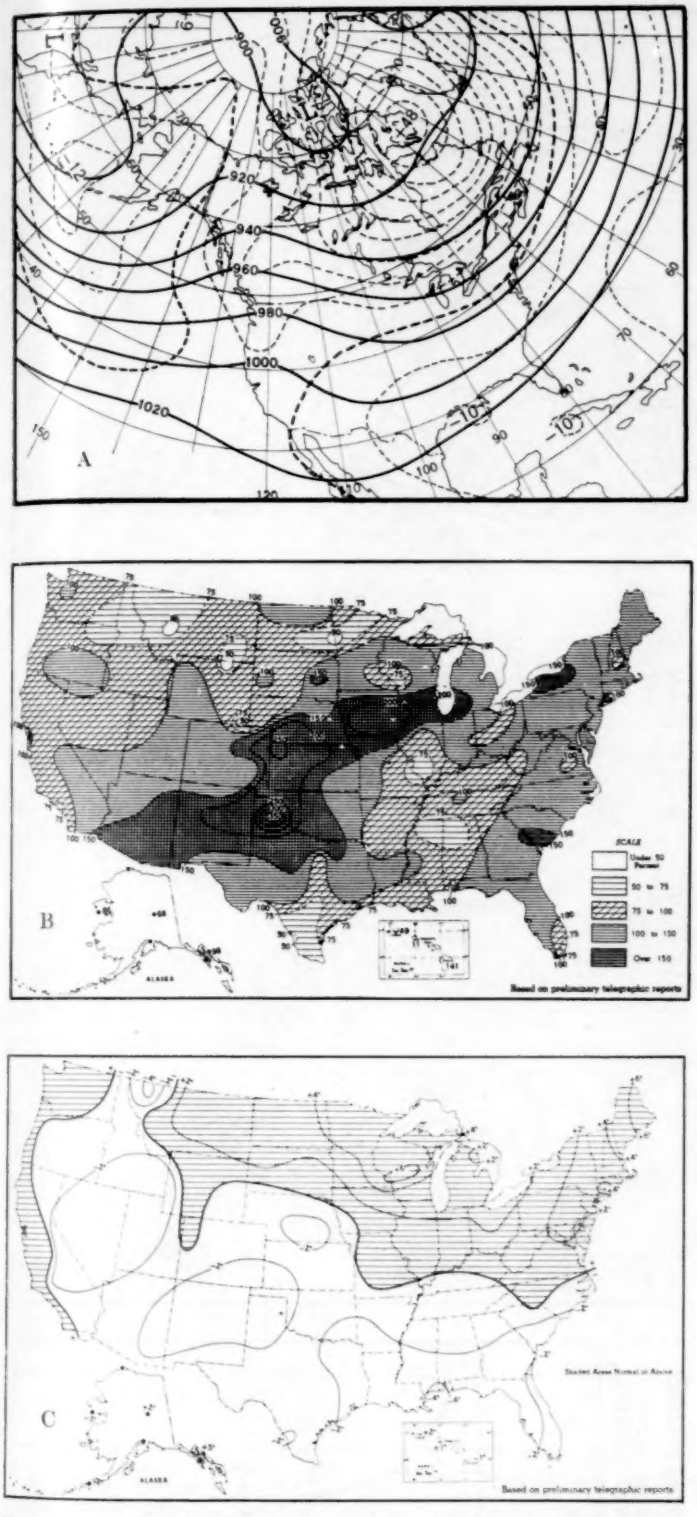

FIGURE 1.—(A) Mean 700-mb. contours (solid) and height departures from normal (dotted) (both in tens of feet) for December 1959–February 1960. The large positive height anomaly in Canada helped define the strong blocking. (B) Percentage of normal precipitation for December 1959–February 1960. Excessive precipitation was widespread and related to numerous daily storms south of the block. (From [8].) (C) Temperature departure from normal (°F.) for December 1959–February 1960. Note the warmth in the North and cold in the South. (From [8].)

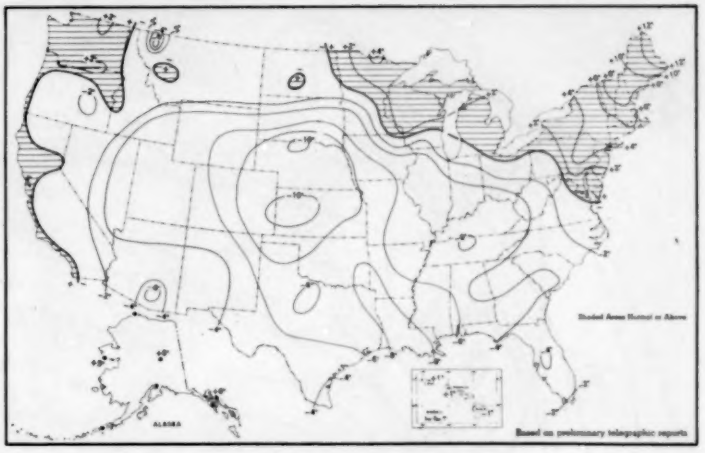

FIGURE 2.—Temperature departure from normal (°F.) for February 1960. Repeated invasions of cold air caused temperatures to average as much as 10° F. below normal in the Central Plains States. (From [8].)

The observed tracks of daily cyclones are illustrated in Chart X of [5] and should be compared with the observed 30-day mean sea level and DN chart (fig. 7). In the Pacific the Aleutian Low and subtropical High were close to their normal positions [6] since that ocean was affected little by the blocking over North America. In the Atlantic, however, the storm tracks were depressed southward, as were the 700-mb. westerlies. There blocking was quite noticeable since sea-level pressures south of 45° N. were less than normal with a maximum departure of −11 mb. near the Azores. The 1004-mb. Low just west of the United Kingdom was evidence of the great displacement of the Icelandic Low, normally located near Cape Farewell, Greenland.

In the United States the Southeast is normally under the influence of a mean High at sea-level. In February, however, that area had an average sea-level pressure as much as 6 mb. lower than normal and was subject to a mean flow from the north (fig. 7). There was an appreciable increase in the frequency and intensity of storms in the eastern United States compared to a long term average [7]. The procession of cyclones east of the Rockies and the frequent occurrence of cold ridges at sea level (see mean ridge in fig. 7) led to a cold, snowy February for much of the Nation.

3. MONTHLY MEAN WEATHER

Monthly mean temperature anomalies in the United States during February (fig. 2) were defined, to a great extent, by the blocking over eastern Canada (fig. 3). Colder than normal temperatures prevailed in at least three-fourths of the country. Negative departures from normal averaged 8 to 10° F. from the Central Plains to the Gulf Coast. In contrast, portions of the northeastern quadrant were above normal with a maximum of +12° F. in Maine.

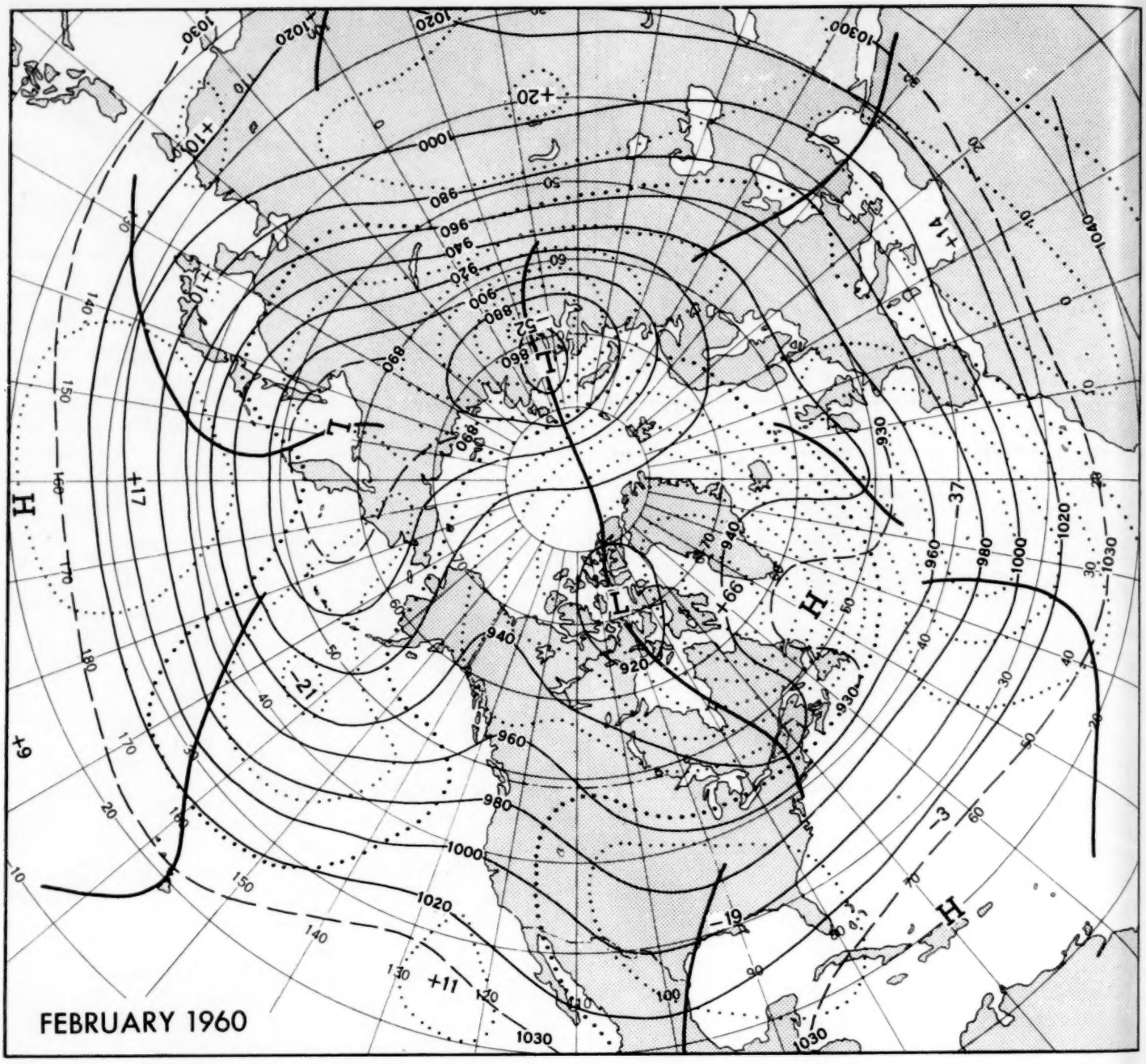

FIGURE 3.—Mean 700-mb. contours (solid) and height departures from normal (dotted) (both in tens of feet) for February 1960. Heavy solid lines are minimum latitude troughs. The expanded circumpolar vortex and high latitude blocking are emphasized particularly well by the height departures.

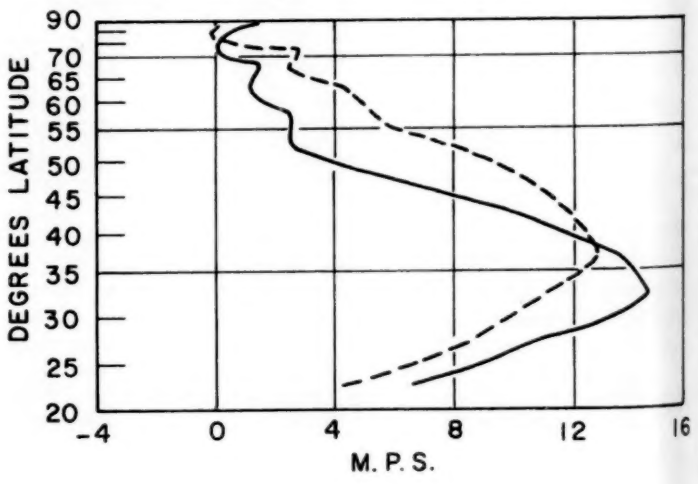

FIGURE 4.—Mean 700-mb. zonal wind speed profiles in the western portion of the Northern Hemisphere for February 1960 (solid) and February normal (dashed). The belt of maximum wind was displaced south of normal as a result of the blocking.

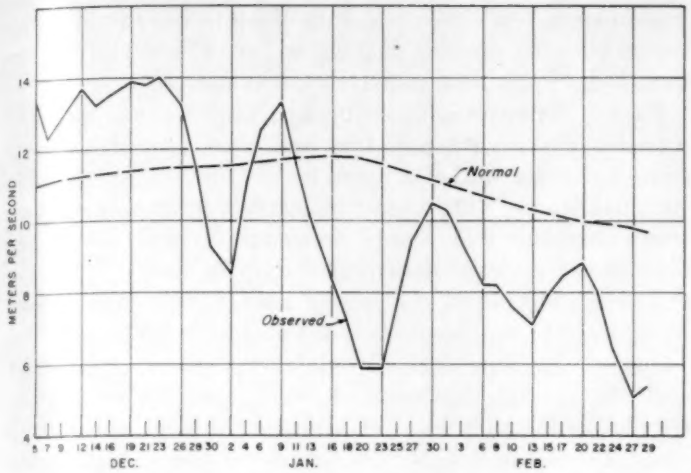

FIGURE 5.—Time variation of zonal index in meters per second for the western portion of the Northern Hemisphere in the latitude zone 35–55°N. The downward trend of the zonal index during the 1959–60 winter season was accompanied by a similar trend of temperature. The lowest index value in February and the coldest 5-day mean temperatures occurred at about the same time.

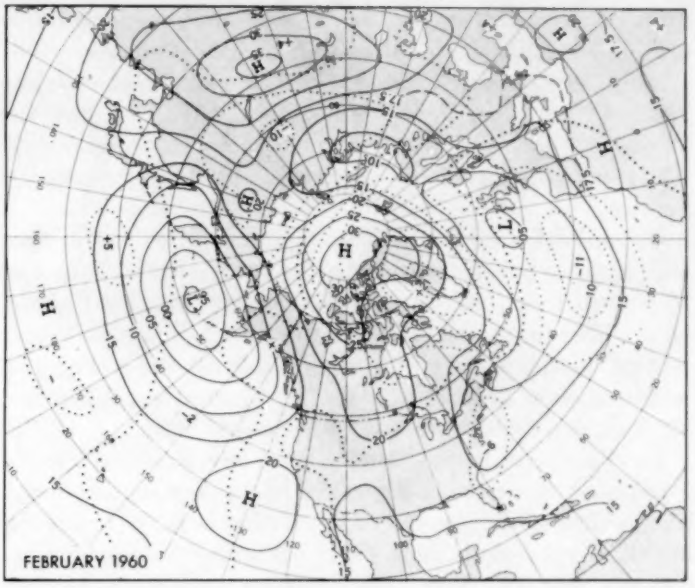

FIGURE 7.—Mean sea-level pressure and departure from normal (both in millibars) for February 1960. The Pacific was not appreciably affected by blocking, but in the Atlantic note the large displacement of the Icelandic Low.

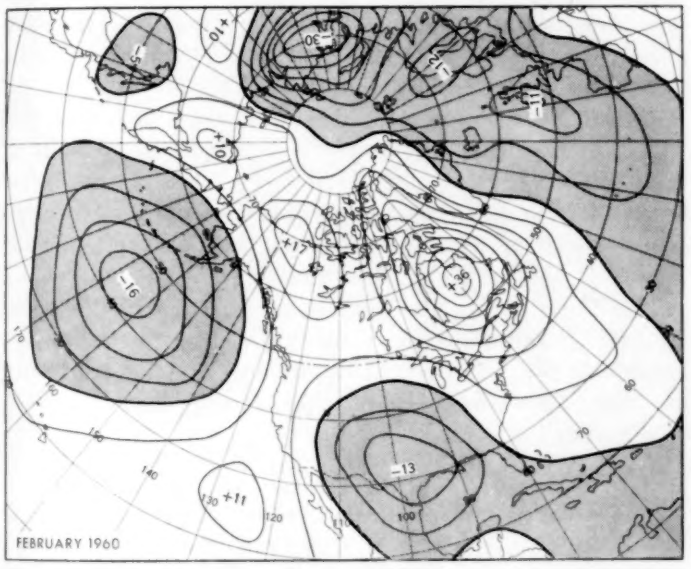

FIGURE 6.—Mean thickness (1000 to 700 mb.) departure from normal (tens of feet) for February 1960. There was a close correspondence between cooler than normal thickness and cooler than normal sea-level temperatures (fig. 2).

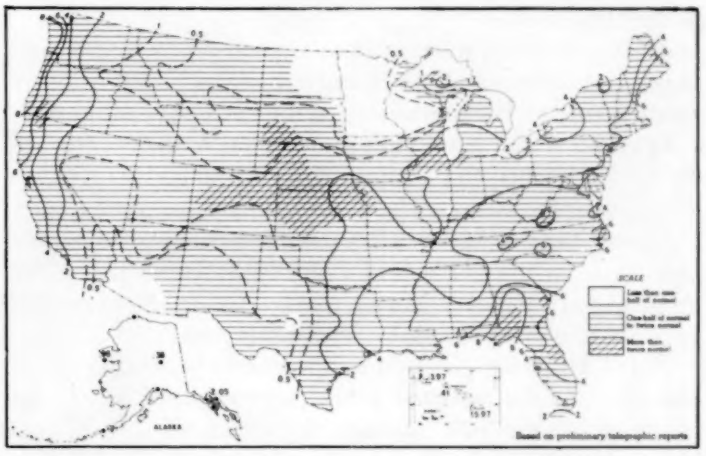

FIGURE 8.—Total precipitation (inches) for February 1960. Much of the precipitation east of the Rockies resulted from record and near-record snowstorms. (From [8].)

The cold portion of the United States was found where 700-mb. heights were generally less than normal and where upper level contours were cyclonic. The warm Northeast was also subject to a cyclonic flow, and since that flow was northwesterly, it would appear to have transported cold air into New England. However, 700-mb. heights were above normal and the DN flow was from an easterly direction, so that onshore advection of relatively warm air from the Atlantic was observed more frequently than normal during February. In fact this circumstance occurred much of the winter season.

The warm temperatures in the Northeast were an extremity of the greater picture which encompassed all the provinces and territories north of the Canadian border. There were no monthly mean temperatures below normal (except for extreme southern Saskatchewan) from Vancouver Island to Ellsmere Island and from Newfoundland to Point Barrow. The westward growth of anticyclogenesis in Canada was concurrent with the widespread warmth just described.

As expected, below normal values of monthly mean 1000 to 700-mb. thickness (fig. 6) practically coincided with below normal surface temperatures in the United

States. Similarly, above normal thickness attended above normal surface temperatures in North America. The +360-ft. center near Labrador was the maximum absolute value in the Northern Hemisphere. It was also the location of the maximum surface temperature anomaly (+24° F.) reported by the Canadian Meteorological Service.

Precipitation amounts exceeding 150 percent of normal (fig. 8) were generally confined to the Central Plains and to a strip from coastal New England to central Florida. In the East four storms west of the Appalachians and three east of the mountains were responsible for the record 27.6 inches of snow at Roanoke, Va., 21.5 inches at Charleston, W. Va., and 20.8 inches at Youngstown, Ohio.

In the Great Plains much of the precipitation can be attributed to overrunning initiated by a storm in north Texas early in the month. Another factor in the mean was cyclonic anomalous flow from an easterly direction at 700 mb. (fig. 3). Furthermore, there were 10 or 11 days with fronts from Montana to western Kansas as Pacific maritime air overran Canadian Polar air. February snowfall records were reported at Goodland, Kans., which had 25.4 inches, Kansas City, Mo., 20.7 inches, and Lincoln, Nebr., 19.2 inches.

Alaska recorded warmer than normal temperatures and normal or subnormal precipitation. The monthly mean temperature at Barrow averaged 9.6° F. above normal for February. A new maximum for the month was established on the 28th when the temperature rose to 32° F. On the same date the temperature at Yakutat reached a new February high of 49° F. Greatest mean temperature departure from normal was +12.0° F. at Kotzebue. The unusual warming over Alaska was related to above normal 700-mb. heights and southeasterly DN flow.

In the Hawaiian Islands temperatures were also rather extreme. Lihue reported a new maximum of 86° F. for February and a new all-time minimum of 53° F. At Honolulu 56° F. was a new low for the month. An all-time minimum of 55° F. was established at Hilo. The new records in the Hawaiian Islands were attained on those days when the normal trade wind regime was absent.

4. A TRANSITION AT MID-MONTH

CIRCULATION

The evolution of the circulation during February cannot be assessed solely from an inspection of the monthly mean charts. Half-monthly mean charts, shown in figure 9, depict clearly the great change which occurred in February, and emphasize its proportions.

First consider figure 9A, the 700-mb. mean for the 15-day period ending February 14. The trough in the central Pacific terminated in an intense Aleutian Low, which was 600 feet below normal. The ridge over North America was relatively weak. Although it was somewhat higher than normal in the United States, it was lower than normal in Canada. The trough downstream had fractured and was weak in the north, but quite deep in the south. Two severe storms deepened in the Southern Plains early in the month, en route to the eastern Great Lakes.

In the Atlantic the most important feature was the division of the westerlies into one branch northeastward from Labrador and the other eastward from the Middle Atlantic States. The height departures from normal show that blocking was firmly entrenched near Labrador, despite the cyclonic nature of the upper flow.

The circulation of the second half of February, shown in figure 9A, represents a drastic change from the first 15 days. Considering only major troughs in figures 9A and 9B, the readjustment of the circulation resulted in the following changes: (1) strengthening of the trough along the Asiatic coast; (2) demise of the trough in the mid-Pacific; (3) retrogression of the trough in the southern United States; (4) development of a new trough in the eastern Atlantic; and (5) effective loss of a trough in Eurasia.

As a result of these changes the hemispheric wave number was reduced by one. Considering both contours and height departures from normal, there were two major troughs at high latitudes and four at middle and lower latitudes in the first 15 days of the month. The wave number was reduced by one at both high and middle latitudes during the last 15 days of February.

In and near North America the change in height DN was of great magnitude and is accentuated graphically in figure 9C. The blocking in eastern Canada intensified by 560 feet and appeared to spread westward. The ridge which had been over the continent was located some 35° longitude to the west. It extended from the sub-tropics to the Polar Basin, the heights increased in the 2 weeks by 1,020 feet in the Gulf of Alaska. That was the largest change in the Northern Hemisphere, and its proximity to North America was of considerable importance to weather in the United States.

WEATHER

The weekly march of cold weather in February is described by the series of temperature departures from normal in figure 10, taken from [8]. For the week ending February 7 (fig. 10A), temperatures were above normal over most of the Nation, with a maximum of 18° F. in North Dakota. Acute cooling in the central portion of the United States in the second week (fig. 10B) followed the development of an intense cyclone which swept across the Rockies from eastern Colorado, where it intensified, to the central Lakes and into Canada (Chart X of [5]). Its passage in the Central and Southern Plains was accompanied by snow, strong winds, and record sea-level pressure for many stations. One of the lowest was 28.70 inches (972 mb.) at Ponca City, Okla. On the day prior to the storm, temperatures in the upper Rio Grande Valley reached as high as 102° F.; two days after the storm's passage, maximum temperatures were in the high 50's in that area.

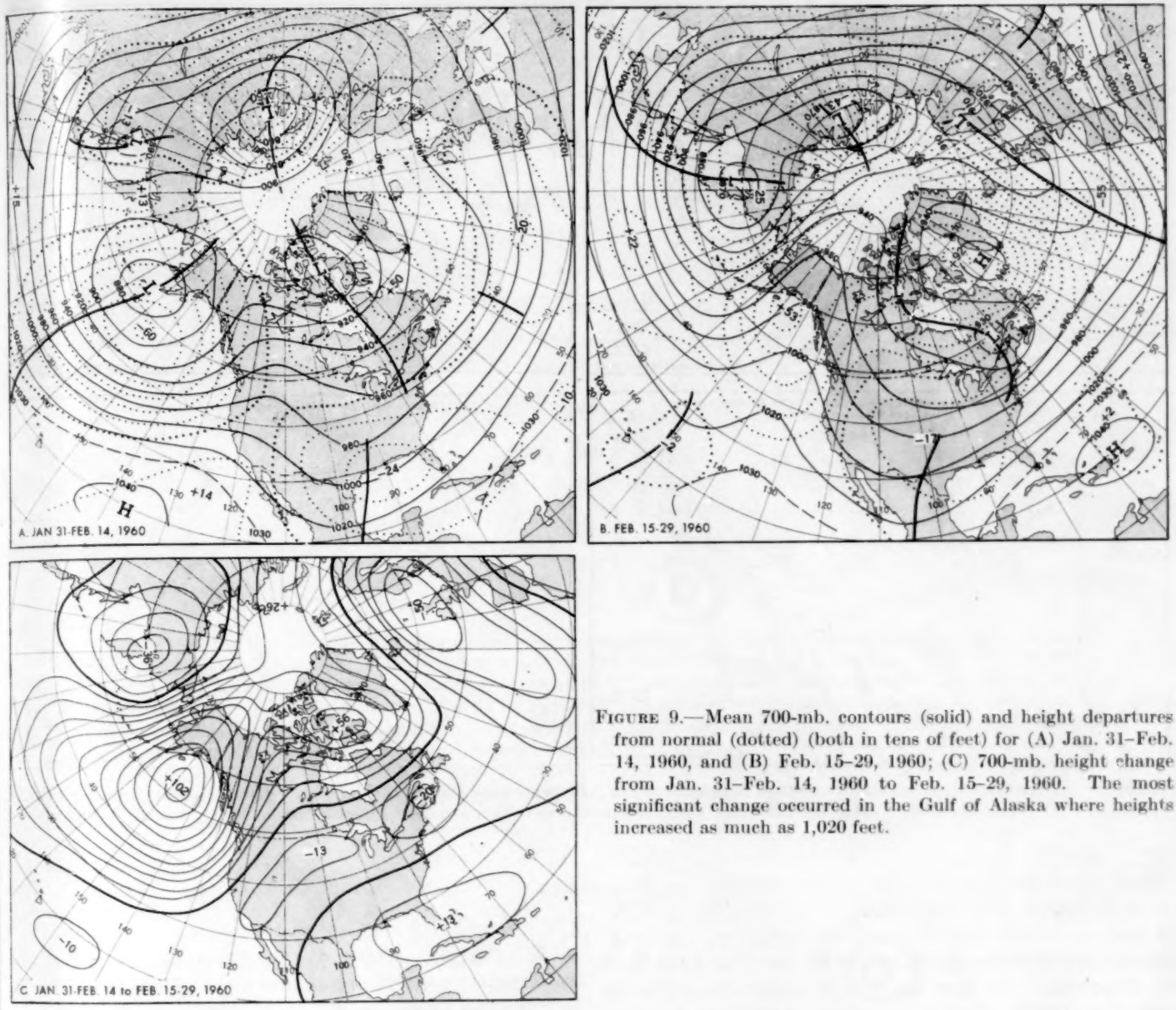

FIGURE 9.—Mean 700-mb. contours (solid) and height departures from normal (dotted) (both in tens of feet) for (A) Jan. 31–Feb. 14, 1960, and (B) Feb. 15–29, 1960; (C) 700-mb. height change from Jan. 31–Feb. 14, 1960 to Feb. 15–29, 1960. The most significant change occurred in the Gulf of Alaska where heights increased as much as 1,020 feet.

The consequences of the change in circulation over North America in the last two weeks of February were pronounced. Figure 9B indicates the strength of the great ridge in the eastern Pacific which propelled cold air into the United States. By the end of the third week (fig. 10C), weekly mean temperatures had dropped as much as 6° F. over a large part of the country. A storm which developed over southeastern Texas on the 17th deepened rapidly as it traversed the Gulf States, crossed the Middle Atlantic States, and moved into the Bay of Fundy. In its wake was a broad band of heavy snowfall from the central Mississippi Valley to the Maritime Provinces.

The continued rise in 700-mb. heights in northwestern North America favored severe cold in most of the United States. The strong northwesterly flow from the Beaufort Sea to the Rocky Mountain States (fig. 9B) was responsible for a prolonged outbreak of Arctic air into the United States. In figure 10D, week ending February 28, temperatures averaged below normal in most of the United States. Mean temperatures more than 20° F. below normal were observed from northern Texas to Montana. Rather weak storms in the southern and central portions and one major storm in the East were responsible for as much as 16 inches of snow in Kansas and lesser amounts to the east.

In all instances just discussed (fig. 10) the most per-

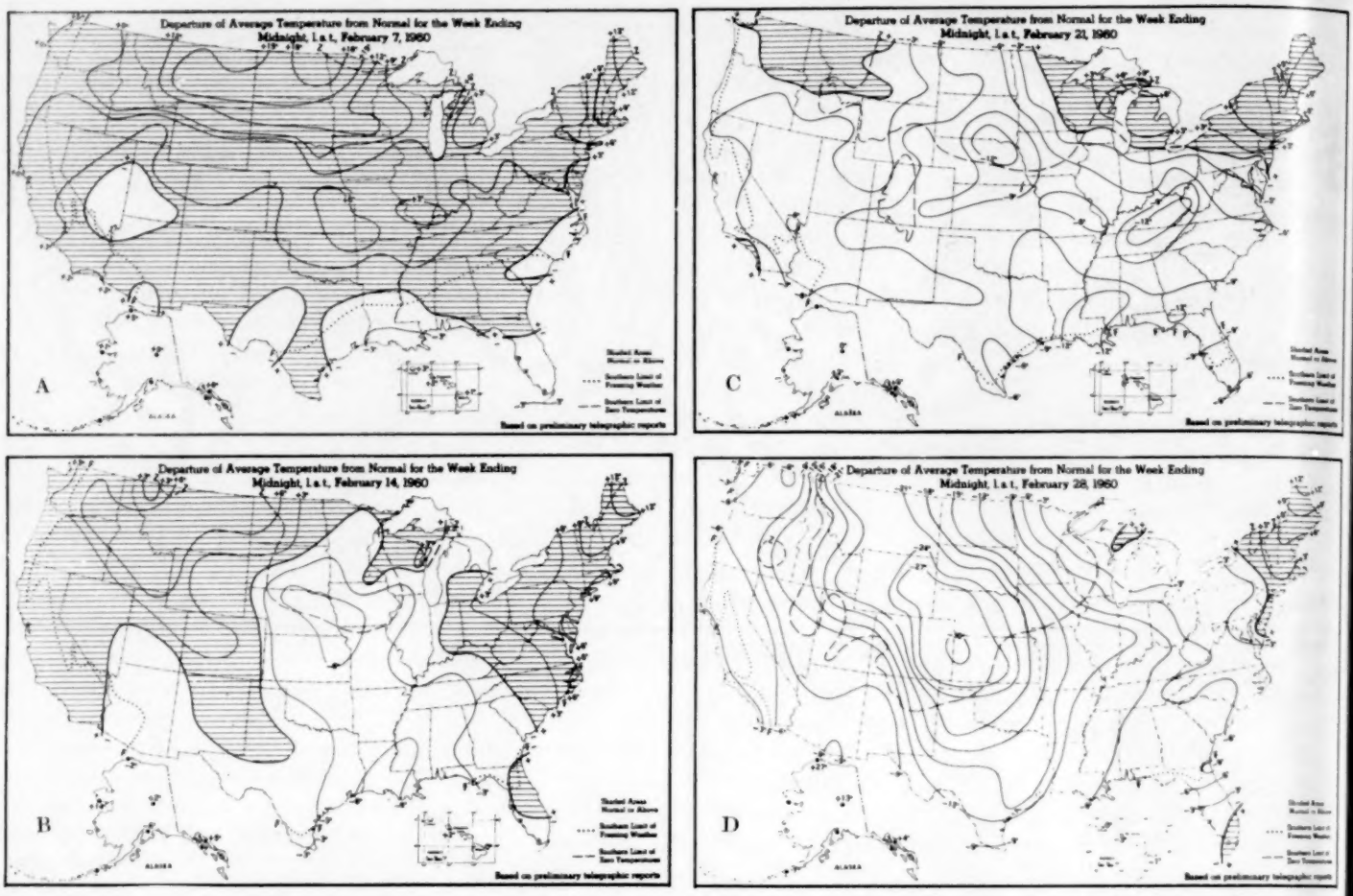
Departure of Average Temperature from Normal for the Week Ending
Midnight, l.s.t., February 7, 1960
A
Departure of Average Temperature from Normal for the Week Ending
Midnight, l.s.t., February 21, 1960
C
Departure of Average Temperature from Normal for the Week Ending
Midnight, l.s.t., February 14, 1960
B
Departure of Average Temperature from Normal for the Week Ending
Midnight, l.s.t., February 28, 1960
D

FIGURE 10.—Departure from normal of average temperature (°F.) for weeks ending (A) Feb. 7, 1960, (B) Feb. 14, 1960, (C) Feb. 21, 1960, and (D) Feb. 28, 1960. After the mild first week, temperatures over a large area became progressively colder. (From [8]).

sistent feature common to all weeks was the warmth in the Northeast. In New England temperatures averaged from 6 to 12° F. warmer than normal each week. This area was influenced by mild Atlantic air under the blocking regime. Thus, while other regions of the country were experiencing cold weather in February, it was an exceptionally mild month in New England.

REFERENCES

1. J. Namias, "The Index Cycle and Its Role in the General Circulation," *Journal of Meteorology*, vol. 7, No. 2, Apr. 1950, pp. 130–139.
2. C. M. Woffinden, "The Weather and Circulation of December 1959—An Abrupt Change from a Cold Fall Season," *Monthly Weather Review*, vol. 87, No. 12, Dec. 1959, pp. 453–458.
3. R. A. Green, "The Weather and Circulation of January 1960–Another January With Atlantic Blocking," *Monthly Weather Review*, vol. 88, No. 1, Jan. 1960, pp. 36–42.
4. H. C. Willett, "Patterns of World Weather Changes," *Transactions*, American Geophysical Union, vol. 29, No. 6, Dec. 1948, pp. 803–809.
5. U.S. Weather Bureau, *Climatological Data—National Summary*, vol. 11, No. 2, Feb. 1960.
6. U.S. Weather Bureau, "Normal Weather Charts for the Northern Hemisphere," *Technical Paper* No. 21, Oct. 1952, 74 pp.
7. W. H. Klein, "Principal Tracks and Mean Frequencies of Cyclones and Anticyclones in the Northern Hemisphere," U.S. Weather Bureau, *Research Paper* No. 40, 1957, 60 pp.
8. U.S. Weather Bureau, *Weekly Weather and Crop Bulletin, National Summary*, vol. XLVII, Nos. 6–12, Feb. 8, 15, 22, 29, Mar. 7, 14, 21, 1960.

U.S. GOVERNMENT PRINTING OFFICE: 1960